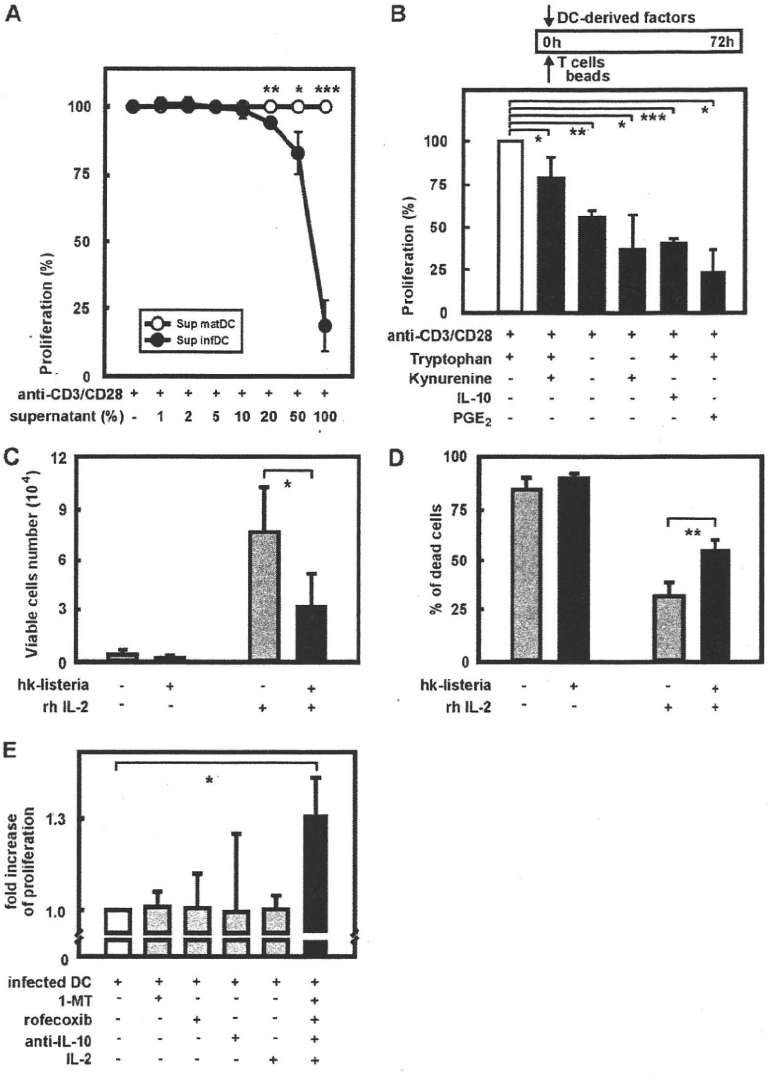

FIGURE 3. Multiple inhibitory pathways must be blocked in infected DC to rescue T cell proliferation. *A*, CFSE-labeled $CD4^+$ T cells were coincubated with anti-CD3 and anti-CD28 beads (beads/T cells ratio 1:1) in CellGro medium supplemented with supernatants, derived from matDC (○) or infDC (●) (in a dilution range from 1 to 100%). In the diagram, percentages of T cells proliferating in infDC-derived supernatants (●) are shown relative to T cells cultured in matDC-derived supernatants (○), taken as 100% (mean ± SD; $n = 4$). *, $p < 0.05$; **, $p < 0.005$; and ***, $p < 0.001$. *B*, $CD4^+$ T cells were coincubated with anti-CD3 and anti-CD28 beads (beads/T cells ratio 1:1) in tryptophan-containing RPMI 1640 medium either alone (white bar) or together with L-kynurenine (5 μg/ml), IL-10 (100 ng/ml), or PGE_2 (1 μg/ml) (black bars). Alternatively, tryptophan-free RPMI 1640 medium with or without L-kynurenine was used. Three days upon the onset of T cell culture, T cell proliferation was assessed by flow cytometry (CFSE) or measuring BrdU incorporation. In the diagram, percentages of proliferating T cells of three independent experiments (relative to the simulation with anti-CD3/CD28 beads (ratio 1:1) in tryptophan-containing RPMI 1640 (white bar), taken as 100%; mean ± SD) are shown. *, $p < 0.05$; **, $p < 0.005$; and ***, $p < 0.001$. *C* and *D*, Analysis of cell proliferation (*C*) and viability (*D*) of the IL-2-dependent cell line CTLL-2. Supernatants from $CD25^+$ DC incubated with heat-killed *L.m.* (hk-listeria, black bars) or from $CD25^-$ nontreated DC (gray bars) were supplemented with rhIL-2 and added to CTLL-2 cells. CTLL-2 cell viability and cell numbers were assessed after 48 h (mean ± SD, $n = 4$). *, $p < 0.05$ and **, $p < 0.005$. *E*, To neutralize the suppressive effect of infected DC, IDO inhibitor 1-methyl-tryptophan (10 μM, Sigma-Aldrich), anti-IL-10 mAb (10 μg/ml), COX-2 inhibitor rofecoxib (10 μM), and rhIL-2 (20 U/ml) were added to the MLR at the time of onset separately or in combination. Increase of T cell proliferation is shown relative to T cell cultures in the presence of infected DC (mean ± SD, $n = 3$). *, $p < 0.05$.

induction of the IDO-associated inhibitory molecules CD25, IL-10, and COX-2 during DC infection. TNF-RI and TNF-RII are expressed in infDC (data not shown), while TNF and IFN-γ are secreted by infected DC with TNF production preceding IFN-γ production (10). Secreted TNF was completely sequestered by anti-TNF mAb (infliximab) and was not blocked by Abs against TNF receptors (anti-TNF-RI, anti-TNF-RII) or IFN-γ (Fig. 4*A*). In contrast, IFN-γ was significantly reduced by neutralization of TNF or blocking of TNF-RI/RII, indicating that IFN-γ acts downstream of TNF receptor signaling in infDC (Fig. 4*B*). To control the experiments addressing regulation of CD25, IL-10, and COX-2, we assessed IDO and kynurenine induction. Blockade of TNF or IFN-γ significantly reduced IDO expression and abrogated kynurenine production and this was mediated by both TNF-RI and TNF-RII signaling (Fig. 4, *C* and *D*). Expression of cell-surface and particularly of soluble CD25 was similarly reduced by the blockade of TNF and TNF-RI/II signaling (Fig. 4, *E* and *F*). However, in contrast to IDO, blockade of IFN-γ did not alter expression of CD25 and secretion of sCD25. This was similarly true for IL-10 secretion (Fig. 4*G*) and COX-2 protein induction (Fig. 4*H*), which were inhibited by blockade of TNF but not by IFN-γ. Dose dependency of TNF-mediated induction of CD25, IL-10, COX-2, and also IDO was demonstrated by increasing doses of infliximab or anti-TNF-R Abs (data not shown). Inhibition of IL-10 or COX-2 did not alter expression of CD25 or IDO (data not shown). Altogether, this places TNF as a central mediator of inhibitory molecules in DC during *L.m.* infection. TNF receptor-mediated signaling is required for induction of IFN-γ, COX-2, IL-10, CD25, and IDO, whereas IFN-γ is only necessary for IDO induction.

Regulatory DC suppress the growth of L.m.

Based on up-regulation of molecules involved in tryptophan metabolism (IDO, KMO, KYNU; see Fig. 1*A*), we postulated that tryptophan reduction might play a role in defense against *L.m.* (32). To assess *Listeria* uptake and bactericidal capacity, we first searched for an appropriate model system. The models were defined by a comparison of comprehensive transcriptional signatures of infected DC, described herein, and of differentially treated DC performed by ourselves or derived from publicly accessible databases, and by a regulatory DC (DCreg) phenotype, which we defined to be CD25/IDO/COX-2 and IL-10. Treatment of immDC with a combination of TNF and Pam_3, as well as with TNF, PGE_2, and Pam_3 (A. Popov, unpublished observations) or LPS (33) (data accessible at NCBI GEO database, accession no. GSE2706, at link provided above) resulted in up-regulation of *IL2RA*, *INDO*, *IL10*, and *PTGS2* as well as genes coding for bactericidal peptides, toxic oxygen, and nitrogen radicals' donors and acidic proteases (data not shown). Moreover, TNF/

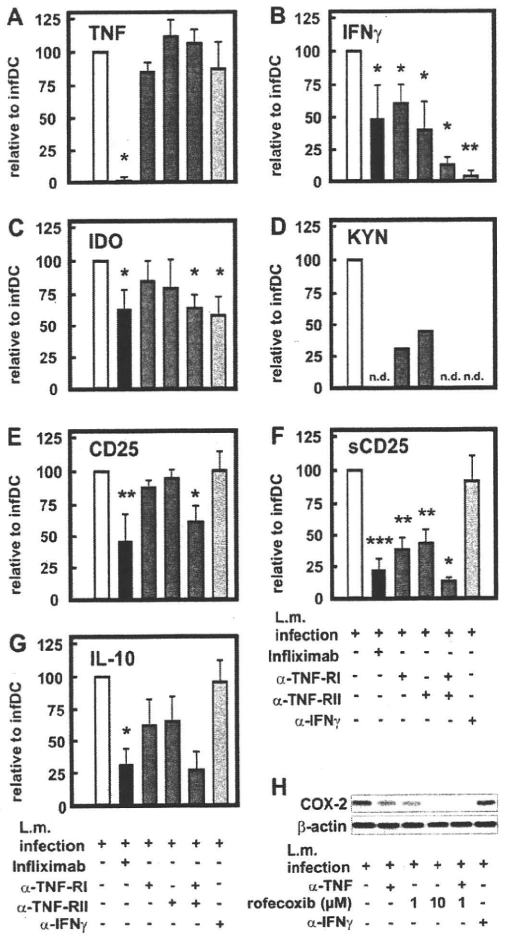

FIGURE 4. Induction of DC with regulatory phenotype is controlled by TNF. Immature DC were infected with wild-type *L.m.* Immediately after infection, DC were incubated with anti-TNF Ab infliximab (1 μg/ml, black bars), anti-TNF-RI (α-TNF-RI), or anti-TNF-RII (α-TNF-RII) mAbs (100 μg/ml, dark gray bars) or anti-IFN-γ mAb (α-IFN-γ, 1 μg/ml, light gray bars). Cells and supernatants were harvested 24 h postinfection. Percentage of reduction was calculated relative to the values derived from DC, infected by wild-type *Listeria*, taken as 100% (white bar). Asterisks highlight the statistically significant comparisons of various treatments vs *Listeria*-infected untreated DC. *A*, Secretion of TNF was measured by ELISA (mean ± SD; at least three independent experiments were performed). *, $p < 0.000005$. *B*, Secretion of IFN-γ was measured by ELISA (mean ± SD; at least three independent experiments were performed). *, $p < 0.05$ and **, $p < 0.00005$. *C*, IDO expression was assessed by flow cytometry as shown in Fig. 1*B* and mean fluorescence intensity values were compared (mean ± SD, $n = 3$). *, $p < 0.05$. *D*, Kynurenine (KYN) accumulation was assessed using a photometric assay. n.d., not detectable. *E*, Analysis of cell-surface expression of CD25 was performed by flow cytometry (mean ± SD; at least three independent experiments were performed). *, $p < 0.05$ and **, $p < 0.005$. *F*, Analysis of sCD25 concentration was performed by ELISA (mean ± SD; at least three independent experiments were performed). *, $p < 0.05$; **, $p < 0.005$; and ***, $p < 0.00005$. *G*, Secretion of IL-10 was measured by ELISA (mean ± SD; $n = 3$ except for combination of anti-TNF-R ($n = 2$)). *, $p < 0.01$. *H*, Protein expression of COX-2 and β-actin (as loading control) was assessed by Western blot. Infected DC were either left untreated or were treated with anti-TNF mAb (α-TNF, 20 μg/ml), COX-2 inhibitor rofecoxib (1–10 μM), or anti-IFN-γ mAb (α-IFN-γ, 1 μg/ml). One representative experiment out of five is shown.

PGE_2/Pam_3 and LPS treatment resulted in the induction of a DCreg phenotype (Fig. 5*A*). To address if a comparable phenotype can be induced in human DC, which are associated with infection foci but are not infected themselves, we incubated immDC or matDC with the supernatants derived from the allogeneic immDC, matDC, or infDC, respectively. All supernatants were double sterile filtered (0.2 μm) and seeded on agar plates to assure the absence of bacteria before the experiment (data not shown). As shown in Fig. 5*B*, incubation of immDC with infDC-derived supernatants, but not with the supernatants derived from immDC or matDC, resulted in the induction of the DCreg phenotype. Comparable results were obtained in a transwell system when immDC (lower chamber) were cocultured with infDC (upper chamber) and when mature DC were treated with the supernatants derived from infected DC (data not shown).

For additional experiments we mostly used $TNF/PGE_2/Pam3$-induced DC as a model for IDO^+ DCreg. Different DC subsets (immDC, matDC, DCreg) were infected with FITC-labeled *L.m.* at a multiplicity of infection of 10 and bacterial burden was analyzed over time after infection. As determined by uptake of bacteria, susceptibility to infection with *L.m.* differed between various DC populations (Fig. 5*C*). As expected, immDC were more easily infected than IDO^- matDC and IDO^+ DCreg. Among the latter two, IDO^+ DCreg were most resistant against infection and phagocytosed less *Listeria* than did matDC. Within the first 30 min after infection, all DC subsets substantially reduced the initial bacterial load; however, on a cell-to-cell basis, IDO^+ DCreg were significantly more efficient in controlling the phagocytosed *Listeria* than IDO^- immDC or IDO^- matDC (Fig. 5*D*, relative number of intracellular viable bacteria derived 30 min after infection and normalized to the initial time point ($t = 0$) set to 100% is shown). Moreover, only IDO^+ DCreg were able to significantly restrict the number of viable intracellular bacteria over time, while the number of viable *L.m* in matDC and immDC significantly increased during the course of infection (Fig. 5*E*). Importantly, DC expressing a regulatory phenotype were equally efficient in "managing" intracellular *Listeria* independently of the factors used for inducing the DCreg phenotype, such as $TNF/PGE_2/Pam_3$, TNF/Pam_3, LPS, or supernatant-treated DCreg (Fig. 5*E* and data not shown). In contrast, immature DC and DC matured with TNF or anti-CD40 appeared to lose the control over the intracellular bacteria (Fig. 5*E* and data not shown). Overall, fewer IDO^+ DCreg are infected by *L.m.* and those infected are more sufficient in reducing and controlling bacterial load, independently of the agents that induce the regulatory phenotype.

To assess the effect of IDO-mediated tryptophan catabolism on *L.m.*, the survival of *L.m.* was determined in vitro under different concentrations of tryptophan and one of its key downstream metabolites, kynurenine. Growth of *L.m.* was influenced both by tryptophan starvation and toxic metabolites (as exemplified for kynurenine), with kynurenine being more potent than tryptophan reduction in suppressing bacterial growth (Fig. 5*F*).

Regulatory phenotype hallmarks DC in human chronic listeriosis in vivo

To address the in vivo relevance of our findings, we examined CD25 and COX-2 expression in lymph node specimens of patients with serologically confirmed cervicoglandular-type listeriosis with suppurative granuloma. These granulomas consist mostly of $S100^+CD11c^+$ DC and, to a lesser extent, of $CD68^+CD11c^+$ macrophages (10). In fact, most of the cells forming the outer border of the granuloma expressed the DC marker S100 and substantial amounts of IDO, CD25, and also COX-2 (Fig. 6*A*). Of note, granuloma-forming DC did not express the DC activation marker CD83 (Fig. 6*A*), supporting the transcriptional data and the

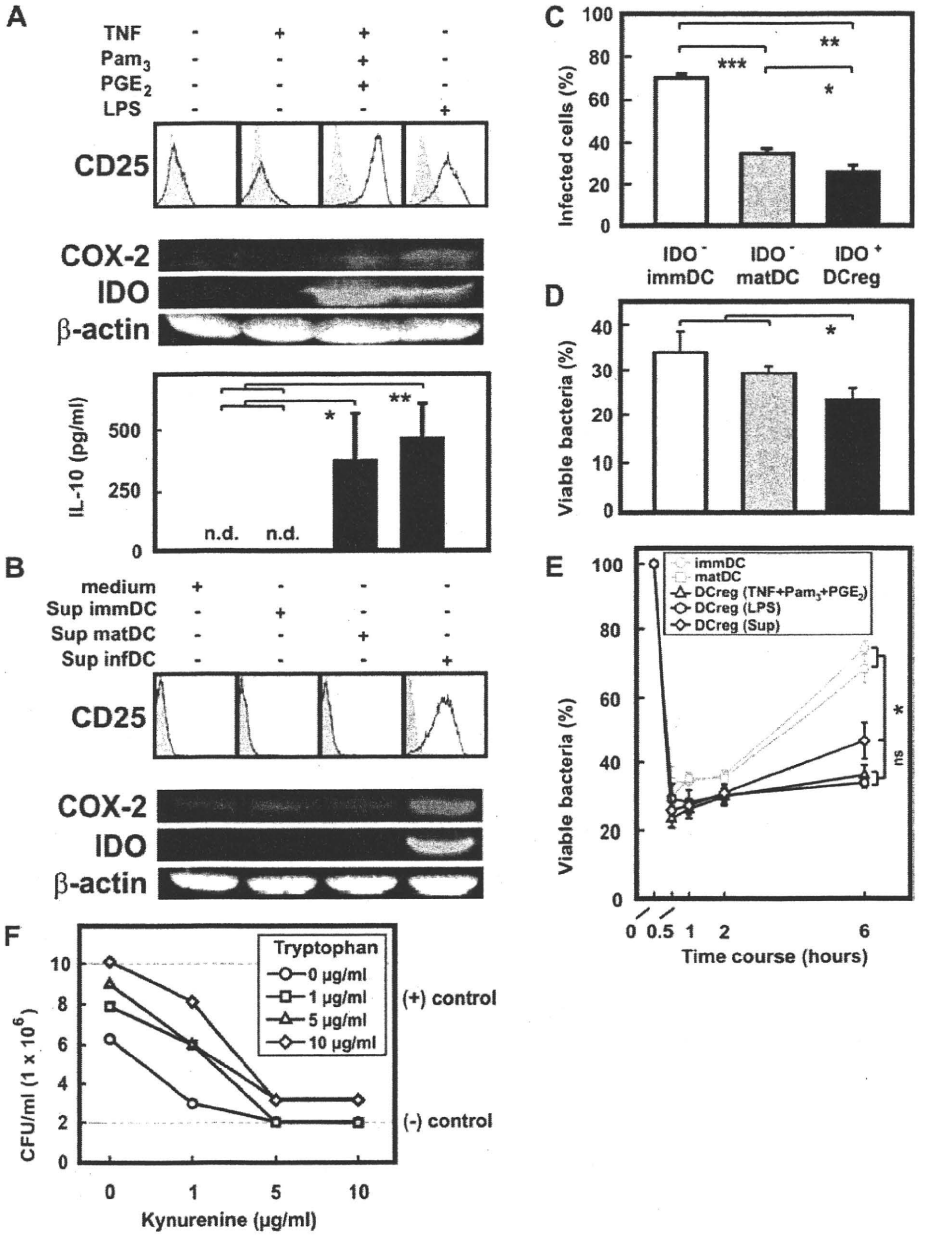

FIGURE 5. Susceptibility of various DC populations for infection with *L.m.* DC were generated from monocytes as described in *Materials and Methods*. IDO^- immDC indicates immature DC; IDO^- matDC, DC matured with TNF; IDO^+ DCreg, DC stimulated with either combination of TNF, PGE_2, and Pam_3, LPS, or supernatants derived from infected DC (Sup). Asterisks highlight the statistically significant comparisons; ns indicates not significant. *A* and *B*, Expression of surface CD25 (flow cytometry) or COX-2 and IDO proteins (Western blot) was assessed in immature DC treated for 3 days with either (*A*) TNF, TNF + PGE_2 + Pam_3, or LPS or (*B*) supernatants derived from immDC, matDC, or infDC (50%). ImmDC, treated with medium alone, and TNF-matured DC were used as controls. Representative experiments are shown; at least four independent experiments were performed per condition. In the lower part of *A*, IL-10 secretion by differentially treated DC assessed by ELISA is shown (mean ± SD, $n = 3$). *, $p < 0.05$; **, $p < 0.01$; and n.d., not detectable. *C*, Infection rates of IDO^- immDC (white bar), IDO^- matDC (gray bar), and IDO^+ DCreg (TNF + PGE_2 + Pam_3, black bar) by FITC-labeled *L.m.* were assessed by flow cytometry after the extracellular bacteria were removed (mean ± SD, $n = 3$). *, $p < 0.05$; **, $p < 0.0005$; and ***, $p < 0.0001$. *D*, Bactericidal activity of IDO^- immDC (white bar), IDO^- matDC (gray bar), and IDO^+ DCreg (TNF + PGE_2 + Pam_3, black bar) infected with *L.m.* was assessed in a CFU assay 30 min after infection. Graph represents the relative number of intracellular viable bacteria derived from DC 30 min after infection (normalized to the initial time point ($t = 0$) set to 100%; mean ± SD, $n = 3$). *, $p < 0.05$. *E*, Bactericidal activity of human DC infected with *L.m.* was assessed over time in a CFU assay. Graph represents kinetics of intracellular viable bacteria at specified time points normalized to the initial time point ($t = 0$) set to 100% (mean ± SD, $n = 3$). *, $p < 0.01$ (between DCreg treated with infDC-derived supernatants and either IDO^- immDC or IDO^- matDC). *F*, *L.m.* was incubated in a tryptophan-free RPMI 1640 medium supplemented with L-tryptophan and L-kynurenine (0–10 µg/ml), and after 6 h the number of *Listeria* was determined as CFU. Negative control, HBSS buffer; positive control, RPMI 1640 medium with tryptophan. Representative experiment with similar results from three independent cultures performed on 3 different days is shown.

results of cell-surface staining (see Fig. 1*B*). Morphological assessment, as well as FoxP3 staining, excluded a massive infiltration of $CD25^+$ regulatory T cells; however, some $FoxP3^+$ cells were present within the granuloma wall and more $FoxP3^+$ cells were detected between the granuloma (Fig. 6*A*). Staining with mAbs specific for CD4, CD8, and CD56 demonstrated that T cells

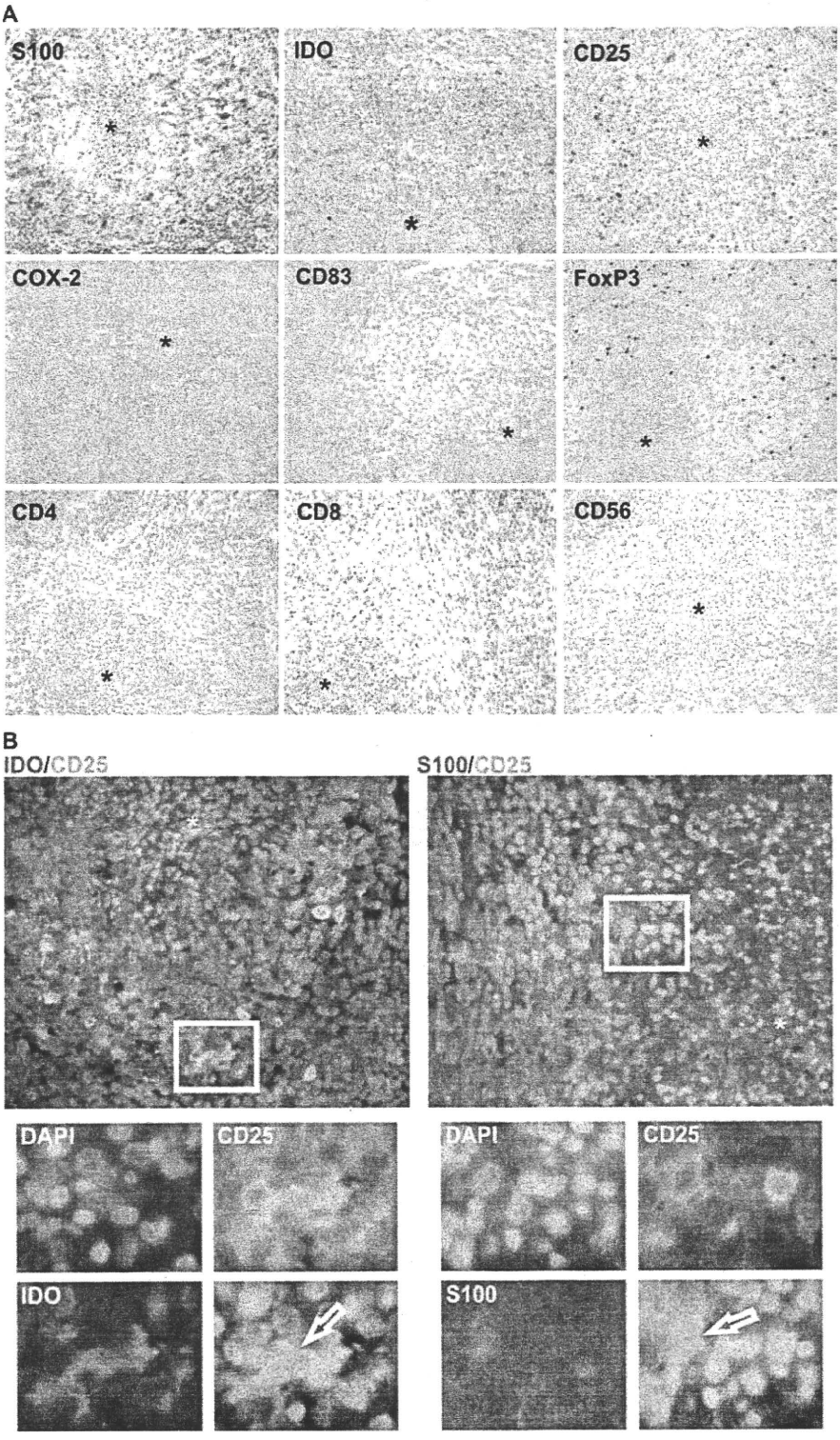

FIGURE 6. DC with regulatory phenotype form the granuloma wall in advanced human listeriosis. Histomorphology of lymph node sections from a patient with cervicoglandular-type suppurative granulomatous listeriosis. One representative case out of three is shown. Asterisks point out the center of granuloma. *A*, Immunohistochemistry of listerial granuloma. Outer ringwall of granuloma in advanced human listeriosis consists of DC (S100). A great majority of cells forming the ringwall around granuloma express IDO and CD25 and stain positive for COX-2, whereas no $CD83^-$ cells are revealed within granuloma ringwall and around granuloma. Single $FoxP3^+$ cells are located within the granuloma wall and outside of the granuloma. $CD4^+$ and $CD8^-$ T cells are located around the granuloma (outside of the ringwall); no $CD56^+$ NK cells are found in the rim or around the granuloma. Magnification, ×250. *B*, Double immmunofluorescence staining for IDO (red, cytoplasmatic staining) and CD25 (green, membrane staining) reveal $CD25^+IDO^+$ cells in granuloma ringwall; magnification, ×400. Double immmunofluorescence staining for S100 (red, cytoplasmatic staining) and CD25 (green) reveal $CD25^+$ DC in granuloma ringwall; magnification, ×400. *Below*, an enlarged section of each photo (marked with a white rectangle; magnification, ×1000) is shown for more detail for every staining separately (DAPI, CD25, and either IDO or S100) and in overlay; double-positive cells (either IDO^+CD25^+ or $CD25^-S100^+$) are highlighted with white arrows.

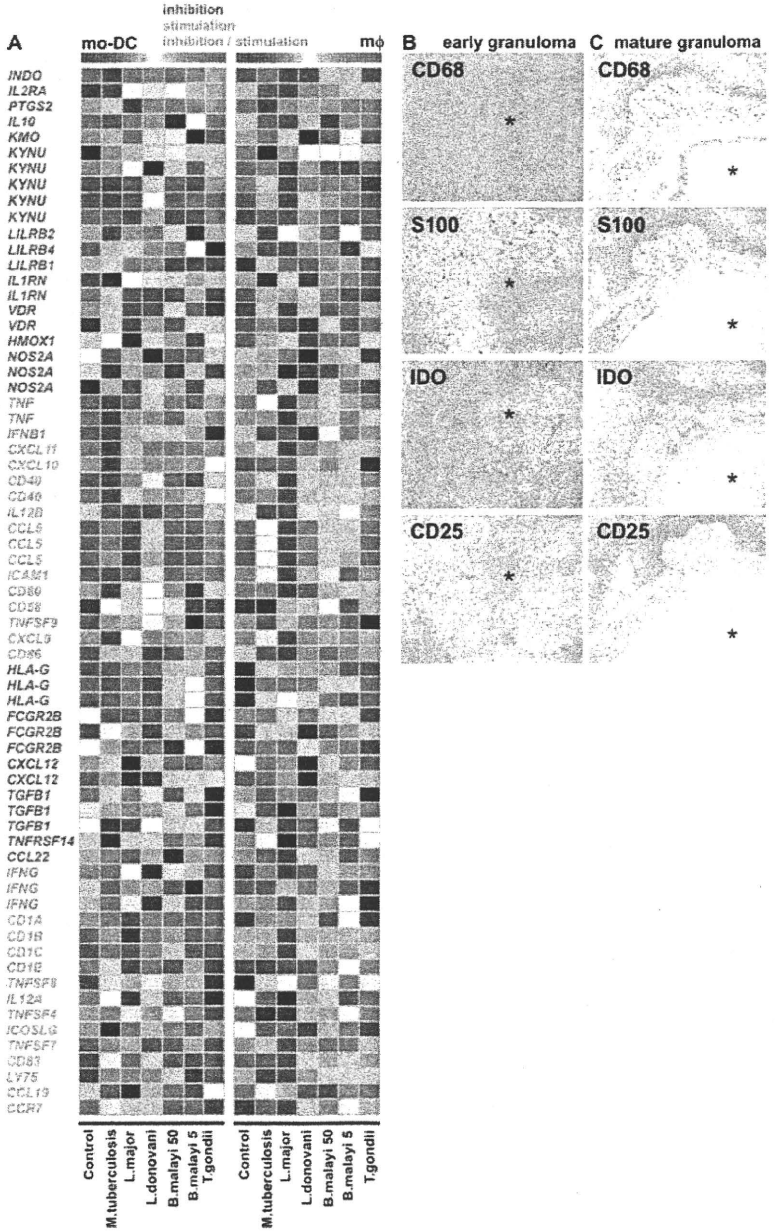

FIGURE 7. Myeloid cells with regulatory phenotype are induced in granuloma during tuberculosis. *A*, Heat map displaying average expression signals of inhibitory and stimulatory genes (Fig. 1*A*). Expression values for mo-DC and macrophages (Mϕ) infected with phylogenetically distinct parasites and bacteria were obtained from NCBI GEO (accession no. GSE360 at http://www.ncbi.nlm.nih.gov/projects/geo/) and average expression signals were standardized (Z score transformation) before visualization. Due to use of a different microarray platform (HG-U95A) several transcripts assessed in Fig. 1*A* (*PDCD1LG2*, *IL23A*, *HMOX1*, *VEGF*, *EBI3*) were not imprinted on the chip and therefore were excluded from the analysis. Transcripts involved in stimulation or inhibition are differentially color-coded. *B*, Immunohistochemistry of early stage granuloma in tuberculosis (*M. tuberculosis*); images of macrophage marker CD68, DC marker S100, IDO, and CD25 were taken at magnification of $\times$100. Asterisks point out the center of granuloma. One representative experiment of three is shown. *C*, Immunohistochemistry of late-stage mature granuloma (same legend as in *B*).

were displaced in the area between the granuloma, whereas NK cells were almost absent. Although we did not perform the costaining of FoxP3 and CD4, based on the spatial localization of both markers, FoxP3$^+$ cells might be regulatory T cells. Using two-color immunofluorescence analysis, we demonstrated that CD25 and IDO are coexpressed by S100$^+$ DC (Fig. 6*B*). Double staining for CD11c and CD25 confirmed CD25$^+$ DC to be of myeloid origin (data not shown). CD68$^+$ macrophages within the granuloma ringwall also expressed CD25, but to a lesser extent as DC (data not shown). Macrophages generated from monocytes and infected with *L.m.* expressed surface CD25, secreted sCD25, and expressed COX-2, albeit to a lesser extent than infDC (data not shown). Altogether, myeloid DC and macrophages within the granuloma express multiple inhibitory molecules associated with a regulatory phenotype of DC (15).

Induction of regulatory DC in other granulomatous infections

If formation and maintenance of granuloma rely on inhibitory pathways induced in myeloid cells, we hypothesized that other pathogens associated with granuloma formation would induce comparable molecular programs. To address this question, we applied the transcriptional signature of stimulatory and inhibitory genes established for *L.m.* infection (see Fig. 1*A*) to a publicly available dataset describing the genome-wide response of human DC and macrophages to phylogenetically distinct pathogens (data accessible at NCBI GEO database, accession no. GSE360, at link provided above) (34). Infection of DC with *M. tuberculosis* and macrophages with *Leishmania major* most closely resembled the expression pattern observed for *L.m.* infection. Induction of transcripts for TNF, IFN-γ, CD25, COX-2, IL-10, and enzymes of the tryptophan catabolism (IDO, KMO, KYNU) was apparent in DC infected with either of these three pathogens (Fig. 7*A*). Similarly, genes encoding stimulatory molecules (e.g., *CD40*, *CD80*, *CD86*, *ICAM1*, and *CD58*) induced in human DC by *L.m.* infection were also induced by *M. tuberculosis* and *L. major*. Other infections assessed in this experiment (Fig. 7*A*) clearly differed in the regulation of stimulatory and inhibitory pathways. To assess the in vivo relevance of these findings, we assessed expression of IDO, CD25,

and COX-2, as well as DC marker S100 and macrophage marker CD68, in granuloma in tuberculosis. The structure of tubercular granuloma is regulated within time: as the granuloma matures, collagen-rich fibers substitute the cells at the periphery, which leads to granuloma organization (35). To determine whether expression of regulatory proteins by granuloma-forming cells is also regulated over time, we examined their expression in the early as well as late-stage granuloma. In contrast to listeriosis, $CD68^+$ macrophages were the major cellular component of early granuloma in tuberculosis, while only few $S100^+$ DC were present; expression of IDO was very prominent and CD25 was moderately expressed (Fig. 7*B*), whereas COX-2 staining was rather faint (data not shown). Costaining experiments revealed that $CD25^+$ cells do express IDO as well as CD11c, confirming their myeloid origin (data not shown). However, regulatory cells seem to be an early event during granuloma formation, since $CD25^+IDO^+$ cells were almost absent in late-stage granuloma, although macrophages and DC were still present (Fig. 7*C*).

Discussion

Tryptophan-catabolizing DC are a major component of granuloma in human listeriosis (10). Herein we demonstrate that granuloma-forming myeloid cells, either DC or macrophages, in human listeriosis and tuberculosis are characterized by coinduction of multiple inhibitory pathways, including CD25 secretion, IL-10 expression, COX-2-dependent mechanisms, as well as tryptophan catabolism. Using listeriosis as a model we linked the induction of this regulatory phenotype of myeloid DC to infection and established TNF as the major mediator of inhibitory proteins, while IFN-γ, which is downstream of TNF, is only required for induction of the tryptophan-catabolizing enzyme IDO. Regulatory DC induced during infection with *L.m.* are strong inhibitors of T cell activation, and their regulatory function can be reversed only by simultaneous blockade of several inhibitory proteins. The modest recovery of T cell proliferation when blocking four regulatory proteins at once (Fig. 3*E*) underscores the predominance of the regulatory DC phenotype over the stimulatory one and points out that even more regulatory mechanisms might be involved (Fig. 1*A*). Regulatory DC are not only endowed with the ability to suppress T cell function, but also to suppress bacterial infection. While tryptophan metabolism in regulatory DC seems to play an important role in reducing bacterial burden during infection, other unknown factors must account for the increased resistance of regulatory DC to infection. Altogether, these findings advocate that regulatory myeloid cells involved in granuloma formation during listeriosis and tuberculosis are provided with multiple inhibitory mechanisms evolved to protect the host from disseminating infection while at the same time inhibiting granuloma destruction by T cells.

Accumulating data suggest that DC, in addition to macrophages, play an important role in the pathogenesis of granulomatous diseases such as listeriosis, tuberculosis, or cat-scratch disease (4, 10, 36, 37). Infection of DC with various pathogens was associated with induction of stimulatory effects on DC function by these pathogens or their components (7, 8, 38). We corroborate these data, demonstrating that important stimulatory molecules (e.g., CD40, CD80, and CD86) are induced in DC and macrophages during infection with *L.m.* and *M. tuberculosis* (Figs. 1 and 7). However, simultaneous induction of several inhibitory pathways (IL-10, COX-2, CD25, and IDO) does counterbalance these stimulatory pathways toward inhibition of T cell function. Furthermore, IL-10 was reported to inhibit pathogen-specific T cell responses (39), and prostaglandins, products of COX-2-mediated arachidonic acid metabolism, were shown to suppress cellular immunity to *Listeria* (40). At the same time both factors directly suppress T cell proliferation (27, 30) and are also involved in the induction of regulatory T cells (41, 42). For CD25, we demonstrated that cell-surface and soluble CD25 induced by infection can function as an IL-2 scavenger receptor. This is in line with clinical evidence linking increased levels of sCD25 to immunosuppression in infectious (43–45) and malignant diseases (46, 47). Of note, induction of CD25 and sCD25, as well as IDO, is not restricted to mo-DC, but has been observed in BDCA-1^+ primary myeloid DC stimulated ex vivo with lipoteichoic acid derived from *L.m.* (A. Popov, unpublished observation) or with PGE_2 (26).

The balance between the stimulatory and inhibitory phenotype of regulatory DC does not result only from the expression of stimulatory or inhibitory molecules, but also from the kinetics of interaction with $CD4^+$ T cells as well as the activation status of the T cells. If the inhibitory phenotype of regulatory DC is elicited before encounter of T cells, their suppressive effect will be clearly more pronounced. Conversely, preactivation of T cells via TCR and costimulatory signals can neutralize the inhibitory effect of regulatory DC.

The bactericidal effect of tryptophan depletion in different cells expressing the key enzymes of the tryptophan pathway has been recognized for several pathogens (32). For *L.m.*, conflicting data concerning the role of tryptophan metabolism have been reported. Although *L.m.* was shown to be auxotrophic for tryptophan (48), growth of the virulent strains of *Listeria* is regarded to be tryptophan independent (49) due to expression of tryptophan synthase genes (*trp*) enabling autonomous tryptophan production (50). Herein we demonstrate that IDO^+ DC are most effective in reducing bacterial burden and infection. Moreover, bacterial growth appears to be predominantly regulated by the accumulation of its toxic metabolite kynurenine. A lower sensitivity to tryptophan starvation compared with the effect of toxic metabolites is in line with previous findings (50). Gram-positive bacteria can produce tryptophan autonomously, making them insensitive to fluctuations in tryptophan concentration in the environment but still vulnerable to the accumulation of toxic metabolites (50). However, IDO^- DC were capable of initially reducing bacterial burden postinfection, suggesting that other mechanisms are utilized by regulatory DC during pathogen containment. Altogether, these data emphasize the importance of tryptophan metabolism for regulatory DC function; however, both T cell suppression as well as pathogen inhibition rely on a multitude of inhibitory mechanisms acting in concert.

An intriguing finding was the hierarchy of signals necessary to induce inhibitory molecules after *Listeria* infection. Clearly, TNF is a main mediator inducing CD25, COX-2, IL-10, and IDO in DC. Furthermore, both TNF receptors are essential for TNF signaling since both had to be blocked to achieve maximum reduction of inhibitory proteins. Most striking, however, was the finding that IFN-γ is clearly downstream of TNF signaling and only governs induction of IDO but not the other inhibitory pathways. The major function of granulomatous structures is the containment of pathogens that otherwise cannot be eradicated by the immune system, thereby preventing an uncontrolled systemic spreading of the pathogen (51, 52). TNF has been recognized as an important factor governing formation and maintenance of granuloma containing intracellular pathogens such as *M. tuberculosis* or *L.m.* (53, 54). However, strict TNF dependency of multiple important inhibitory mechanisms in regulatory DC came somewhat as a surprise since this might be the granuloma's Achilles' heel. Clinical evidence is in line with our experimental data. In patients with rheumatoid arthritis elevated sCD25 serum levels are significantly reduced after treatment with the TNF-neutralizing drug infliximab (55). Suppression of IDO and IL-10 during infliximab therapy was recently

reported for patients with Crohn's disease (56, 57). More dramatic, a severe side effect of anti-TNF therapy is in fact exacerbation of granulomatous listeriosis or tuberculosis mediated by T cells destroying the granulomas (58, 59).

Collectively, this study provides strong evidence that intracellular pathogens such as *M. tuberculosis* and *L.m.* induce a specific transcriptional program in myeloid DC and macrophages characterized by a functional preponderance of multiple inhibitory mechanisms. On the one hand, these myeloid regulatory cells are equipped to suppress unwanted T cell attacks against granulomatous structures; on the other hand, they prohibit pathogens from spreading throughout the host. The exact mechanisms, however, should be studied in the proper animal models. Of particular interest for further research will be the exploitation of the yet unknown pathways of myeloid regulatory cells conferring resistance to infection. This might lead to the discovery of novel strategies protecting other cells from overwhelming infection with these devastating intracellular pathogens.

Acknowledgments

We thank our colleagues from the Center for Transfusion Medicine for providing us with peripheral blood products, and we are grateful to all blood donors. We thank Mirela Stecki and Julia Claasen for technical assistance. We are in debt to Dr. Alexander Poyarkov for his invaluable help during the study design and manuscript preparation. We also thank Drs. K. Schrör and J. Meyer-Kirchrath from the Institute for Pharmacology and Clinical Pharmacology, University of Düsseldorf, Germany, for providing rofecoxib, and Daniela Eggle for critical reading of the manuscript.

Disclosures

The authors have no financial conflicts of interest.

References

1. Pamer, E. G. 2004. Immune responses to *Listeria monocytogenes*. *Nat. Rev. Immunol.* 4: 812–823.
2. Flynn, J. L., and J. Chan. 2001. Immunology of tuberculosis. *Annu. Rev. Immunol.* 19: 93–129.
3. Grivennikov, S. I., A. V. Tumanov, D. J. Liepinsh, A. A. Kruglov, B. I. Marakusha, A. N. Shakhov, T. Murakami, L. N. Drutskaya, I. Forster, B. E. Clausen, et al. 2005. Distinct and nonredundant in vivo functions of TNF produced by T cells and macrophages/neutrophils: protective and deleterious effects. *Immunity* 22: 93–104.
4. Tsai, M. C., S. Chakravarty, G. Zhu, J. Xu, K. Tanaka, C. Koch, J. Tufariello, J. Flynn, and J. Chan. 2006. Characterization of the tuberculous granuloma in murine and human lungs: cellular composition and relative tissue oxygen tension. *Cell Microbiol.* 8: 218–232.
5. Serbina, N. V., T. P. Salazar-Mather, C. A. Biron, W. A. Kuziel, and E. G. Pamer. 2003. TNF/iNOS-producing dendritic cells mediate innate immune defense against bacterial infection. *Immunity* 19: 59–70.
6. Alaniz, R. C., S. Sandall, E. K. Thomas, and C. B. Wilson. 2004. Increased dendritic cell numbers impair protective immunity to intracellular bacteria despite augmenting antigen-specific $CD8^+$ T lymphocyte responses. *J. Immunol.* 172: 3725–3735.
7. Kolb-Maurer, A., I. Gentschev, H. W. Fries, F. Fiedler, E. B. Brocker, E. Kampgen, and W. Goebel. 2000. *Listeria monocytogenes*-infected human dendritic cells: uptake and host cell response. *Infect. Immun.* 68: 3680–3688.
8. Paschen, A., K. E. Dittmar, R. Grenningloh, M. Rohde, D. Schadendorf, E. Domann, T. Chakraborty, and S. Weiss. 2000. Human dendritic cells infected by *Listeria monocytogenes*: induction of maturation, requirements for phagolysosomal escape and antigen presentation capacity. *Eur. J. Immunol.* 30: 3447–3456.
9. de Graaff, P. M., E. C. de Jong, T. M. van Capel, M. E. van Dijk, P. J. Roholl, J. Boes, W. Luytjes, J. L. Kimpen, and G. M. van Bleek. 2005. Respiratory syncytial virus infection of monocyte-derived dendritic cells decreases their capacity to activate CD4 T cells. *J. Immunol.* 175: 5904–5911.
10. Popov, A., Z. Abdullah, C. Wickenhauser, T. Saric, J. Driesen, F. G. Hanisch, E. Domann, E. L. Raven, O. Dehus, C. Hermann, et al. 2006. Indoleamine 2,3-dioxygenase-expressing dendritic cells form suppurative granulomas following *Listeria monocytogenes* infection. *J. Clin. Invest.* 116: 3160–3170.
11. Poncini, C. V., C. D. Alba Soto, E. Batalla, M. E. Solana, and S. M. Gonzalez Cappa. 2008. *Trypanosoma cruzi* induces regulatory dendritic cells in vitro. *Infect. Immun.* 76: 2633–2641.
12. Wong, K. A., and A. Rodriguez. 2008. *Plasmodium* infection and endotoxic shock induce the expansion of regulatory dendritic cells. *J. Immunol.* 180: 716–726.
13. Banchereau, J., and R. M. Steinman. 1998. Dendritic cells and the control of immunity. *Nature* 392: 245–252.
14. Munn, D. H., M. D. Sharma, J. R. Lee, K. G. Jhaver, T. S. Johnson, D. B. Keskin, B. Marshall, P. Chandler, S. J. Antonia, R. Burgess, et al. 2002. Potential regulatory function of human dendritic cells expressing indoleamine 2,3-dioxygenase. *Science* 297: 1867–1870.
15. Morelli, A. E., and A. W. Thomson. 2007. Tolerogenic dendritic cells and the quest for transplant tolerance. *Nat. Rev. Immunol.* 7: 610–621.
16. Steinman, R. M., D. Hawiger, and M. C. Nussenzweig. 2003. Tolerogenic dendritic cells. *Annu. Rev. Immunol.* 21: 685–711.
17. Popov, A., and J. L. Schultze. 2008. IDO-expressing regulatory dendritic cells in cancer and chronic infection. *J. Mol. Med.* 86: 145–160.
18. Jonuleit, H., E. Schmitt, G. Schuler, J. Knop, and A. H. Enk. 2000. Induction of interleukin 10-producing, nonproliferating $CD4^+$ T cells with regulatory properties by repetitive stimulation with allogeneic immature human dendritic cells. *J. Exp. Med.* 192: 1213–1222.
19. Kalinski, P., C. M. Hilkens, A. Snijders, F. G. Snijdewint, and M. L. Kapsenberg. 1997. IL-12-deficient dendritic cells, generated in the presence of prostaglandin E_2, promote type 2 cytokine production in maturing human naive T helper cells. *J. Immunol.* 159: 28–35.
20. Selenko-Gebauer, N., O. Majdic, A. Szekeres, G. Hofler, E. Guthann, U. Korthauer, G. Zlabinger, P. Steinberger, W. F. Pickl, H. Stockinger, et al. 2003. B7–H1 (programmed death-1 ligand) on dendritic cells is involved in the induction and maintenance of T cell anergy. *J. Immunol.* 170: 3637–3644.
21. Ghiringhelli, F., P. E. Puig, S. Roux, A. Parcellier, E. Schmitt, E. Solary, G. Kroemer, F. Martin, B. Chauffert, and L. Zitvogel. 2005. Tumor cells convert immature myeloid dendritic cells into TGF-β-secreting cells inducing $CD4^+CD25^+$ regulatory T cell proliferation. *J. Exp. Med.* 202: 919–929.
22. Munn, D. H., and A. L. Mellor. 2007. Indoleamine 2,3-dioxygenase and tumor-induced tolerance. *J. Clin. Invest.* 117: 1147–1154.
23. Puccetti, P., and U. Grohmann. 2007. IDO and regulatory T cells: a role for reverse signalling and non-canonical NF-κB activation. *Nat. Rev. Immunol.* 7: 817–823.
24. Sharma, M. D., B. Baban, P. Chandler, D. Y. Hou, N. Singh, H. Yagita, M. Azuma, B. R. Blazar, A. L. Mellor, and D. H. Munn. 2007. Plasmacytoid dendritic cells from mouse tumor-draining lymph nodes directly activate mature Tregs via indoleamine 2,3-dioxygenase. *J. Clin. Invest.* 117: 2570–2582.
25. Takikawa, O., T. Kuroiwa, F. Yamazaki, and R. Kido. 1988. Mechanism of interferon-gamma action. Characterization of indoleamine 2,3-dioxygenase in cultured human cells induced by interferon-gamma and evaluation of the enzyme-mediated tryptophan degradation in its anticellular activity. *J. Biol. Chem.* 263: 2041–2048.
26. von Bergwelt-Baildon, M. S., A. Popov, T. Saric, J. Chemnitz, S. Classen, M. S. Stoffel, F. Fiore, U. Roth, M. Beyer, S. Debey, et al. 2006. CD25 and indoleamine 2,3-dioxygenase are up-regulated by prostaglandin E_2 and expressed by tumor-associated dendritic cells in vivo: additional mechanisms of T-cell inhibition. *Blood* 108: 228–237.
27. Chemnitz, J. M., J. Driesen, S. Classen, J. L. Riley, S. Debey, M. Beyer, A. Popov, T. Zander, and J. L. Schultze. 2006. Prostaglandin E_2 impairs $CD4^+$ T cell activation by inhibition of lck: implications in Hodgkin's lymphoma. *Cancer Res.* 66: 1114–1122.
28. Zakharova, M., and H. K. Ziegler. 2005. Paradoxical anti-inflammatory actions of TNF-α: inhibition of IL-12 and IL-23 via TNF receptor 1 in macrophages and dendritic cells. *J. Immunol.* 175: 5024–5033.
29. Iezzi, G., K. Karjalainen, and A. Lanzavecchia. 1998. The duration of antigenic stimulation determines the fate of naive and effector T cells. *Immunity* 8: 89–95.
30. Groux, H., M. Bigler, J. E. de Vries, and M. G. Roncarolo. 1996. Interleukin-10 induces a long-term antigen-specific anergic state in human $CD4^+$ T cells. *J. Exp. Med.* 184: 19–29.
31. Velten, F. W., F. Rambow, P. Metharom, and S. Goerdt. 2007. Enhanced T-cell activation and T-cell-dependent IL-2 production by $CD83^+$, $CD25^{high}$, $CD43^{high}$ human monocyte-derived dendritic cells. *Mol. Immunol.* 44: 1555–1561.
32. MacKenzie, C. R., K. Heseler, A. Muller, and W. Daubener. 2007. Role of indoleamine 2,3-dioxygenase in antimicrobial defence and immuno-regulation: tryptophan depletion versus production of toxic kynurenines. *Curr. Drug Metab.* 8: 237–244.
33. Napolitani, G., A. Rinaldi, F. Bertoni, F. Sallusto, and A. Lanzavecchia. 2005. Selected Toll-like receptor agonist combinations synergistically trigger a T helper type 1-polarizing program in dendritic cells. *Nat. Immunol.* 6: 769–776.
34. Chaussabel, D., R. T. Semnani, M. A. McDowell, D. Sacks, A. Sher, and T. B. Nutman. 2003. Unique gene expression profiles of human macrophages and dendritic cells to phylogenetically distinct parasites. *Blood* 102: 672–681.
35. Cosma, C. L., D. R. Sherman, and L. Ramakrishnan. 2003. The secret lives of the pathogenic mycobacteria. *Annu. Rev. Microbiol.* 57: 641–676.
36. Uehira, K., R. Amakawa, T. Ito, K. Tajima, S. Naitoh, Y. Ozaki, T. Shimizu, K. Yamaguchi, Y. Uemura, H. Kitajima, et al. 2002. Dendritic cells are decreased in blood and accumulated in granuloma in tuberculosis. *Clin. Immunol.* 105: 296–303.
37. Vermi, W., F. Facchetti, E. Riboldi, H. Heine, S. Scutera, S. Stornello, D. Ravarino, P. Cappello, M. Giovarelli, R. Badolato, et al. 2006. Role of dendritic cell-derived CXCL13 in the pathogenesis of *Bartonella henselae* B-rich granuloma. *Blood* 107: 454–462.
38. Hertz, C. J., S. M. Kiertscher, P. J. Godowski, D. A. Bouis, M. V. Norgard, M. D. Roth, and R. L. Modlin. 2001. Microbial lipopeptides stimulate dendritic cell maturation via Toll-like receptor 2. *J. Immunol.* 166: 2444–2450.
39. Biswas, P. S., V. Pedicord, A. Ploss, E. Menet, I. Leiner, and E. G. Pamer. 2007. Pathogen-specific CD8 T cell responses are directly inhibited by IL-10. *J. Immunol.* 179: 4520–4528.

40. Petit, J. C., G. Richard, B. Burghoffer, and G. L. Daguet. 1985. Suppression of cellular immunity to *Listeria monocytogenes* by activated macrophages: mediation by prostaglandins. *Infect. Immun.* 49: 383–388.
41. Levings, M. K., S. Gregori, E. Tresoldi, S. Cazzaniga, C. Bonini, and M. G. Roncarolo. 2005. Differentiation of Tr1 cells by immature dendritic cells requires IL-10 but not $CD25^+CD4^+$ Tr cells. *Blood* 105: 1162–1169.
42. Sharma, S., S. C. Yang, L. Zhu, K. Reckamp, B. Gardner, F. Baratelli, M. Huang, R. K. Batra, and S. M. Dubinett. 2005. Tumor cyclooxygenase-2/prostaglandin E_2-dependent promotion of FOXP3 expression and $CD4^+$ $CD25^+$ T regulatory cell activities in lung cancer. *Cancer Res.* 65: 5211–5220.
43. Toossi, Z., J. R. Sedor, J. P. Lapurga, R. J. Ondash, and J. J. Ellner. 1990. Expression of functional interleukin 2 receptors by peripheral blood monocytes from patients with active pulmonary tuberculosis. *J. Clin. Invest.* 85: 1777–1784.
44. Barral-Netto, M., A. Barral, S. B. Santos, E. M. Carvalho, R. Badaro, H. Rocha, S. G. Reed, and W. D. Johnson, Jr. 1991. Soluble IL-2 receptor as an agent of serum-mediated suppression in human visceral leishmaniasis. *J. Immunol.* 147: 281–284.
45. Makis, A. C., E. Galanakis, E. C. Hatzimichael, Z. L. Papadopoulou, A. Siamopoulou, and K. L. Bourantas. 2005. Serum levels of soluble interleukin-2 receptor alpha (sIL-2Rα) as a predictor of outcome in brucellosis. *J. Infect.* 51: 206–210.
46. Sheibani, K., C. D. Winberg, S. van de Velde, D. W. Blayney, and H. Rappaport. 1987. Distribution of lymphocytes with interleukin-2 receptors (TAC antigens) in reactive lymphoproliferative processes, Hodgkin's disease, and non-Hodgkin's lymphomas: an immunohistologic study of 300 cases. *Am. J. Pathol.* 127: 27–37.
47. Janik, J. E., J. C. Morris, S. Pittaluga, K. McDonald, M. Raffeld, E. S. Jaffe, N. Grant, M. Gutierrez, T. A. Waldmann, and W. H. Wilson. 2004. Elevated serum-soluble interleukin-2 receptor levels in patients with anaplastic large cell lymphoma. *Blood* 104: 3355–3357.
48. Herbert, K. C., and S. J. Foster. 2001. Starvation survival in *Listeria monocytogenes*: characterization of the response and the role of known and novel components. *Microbiology* 147: 2275–2284.
49. Marquis, H., H. G. Bouwer, D. J. Hinrichs, and D. A. Portnoy. 1993. Intracytoplasmic growth and virulence of *Listeria monocytogenes* auxotrophic mutants. *Infect. Immun.* 61: 3756–3760.
50. Gutierrez-Preciado, A., R. A. Jensen, C. Yanofsky, and E. Merino. 2005. New insights into regulation of the tryptophan biosynthetic operon in Gram-positive bacteria. *Trends Genet.* 21: 432–436.
51. Kaufmann, S. H. 1993. Immunity to intracellular bacteria. *Annu. Rev. Immunol.* 11: 129–163.
52. Tufariello, J. M., J. Chan, and J. L. Flynn. 2003. Latent tuberculosis: mechanisms of host and bacillus that contribute to persistent infection. *Lancet Infect. Dis.* 3: 578–590.
53. Kindler, V., A. P. Sappino, G. E. Grau, P. F. Piguet, and P. Vassalli. 1989. The inducing role of tumor necrosis factor in the development of bactericidal granulomas during BCG infection. *Cell* 56: 731–740.
54. Ehlers, S., C. Holscher, S. Scheu, C. Tertilt, T. Hehlgans, J. Suwinski, R. Endres, and K. Pfeffer. 2003. The lymphotoxin β receptor is critically involved in controlling infections with the intracellular pathogens *Mycobacterium tuberculosis* and *Listeria monocytogenes*. *J. Immunol.* 170: 5210–5218.
55. Kuuliala, A., R. Nissinen, H. Kautiainen, H. Repo, and M. Leirisalo-Repo. 2006. Low circulating soluble interleukin 2 receptor level predicts rapid response in patients with refractory rheumatoid arthritis treated with infliximab. *Ann. Rheum. Dis.* 65: 26–29.
56. Wolf, A. M., D. Wolf, H. Rumpold, A. R. Moschen, A. Kaser, P. Obrist, D. Fuchs, G. Brandacher, C. Winkler, K. Geboes, P. Rutgeerts, and H. Tilg. 2004. Overexpression of indoleamine 2,3-dioxygenase in human inflammatory bowel disease. *Clin. Immunol.* 113: 47–55.
57. Detkova, Z., V. Kupcova, M. Prikazska, L. Turecky, S. Weissova, and E. Jahnova. 2003. Different patterns of serum interleukin 10 response to treatment with anti-tumor necrosis factor α antibody (infliximab) in Crohn's disease. *Physiol. Res.* 52: 95–100.
58. Keane, J., S. Gershon, R. P. Wise, E. Mirabile-Levens, J. Kasznica, W. D. Schwieterman, J. N. Siegel, and M. M. Braun. 2001. Tuberculosis associated with infliximab, a tumor necrosis factor α-neutralizing agent. *N. Engl. J. Med.* 345: 1098–1104.
59. Slifman, N. R., S. K. Gershon, J. H. Lee, E. T. Edwards, and M. M. Braun. 2003. *Listeria monocytogenes* infection as a complication of treatment with tumor necrosis factor α-neutralizing agents. *Arthritis Rheum.* 48: 319–324.

Tohoku J. Exp. Med., 2008, **215**, 43-54

Juzen-taiho-to, an Herbal Medicine, Activates and Enhances Phagocytosis in Microglia/Macrophages

HUAYAN LIU,[1,2] JUN WANG,[1,2] ATSUO SEKIYAMA[1] and TAKESHI TABIRA[1]

[1]Department of Vascular Dementia Research, National Institute for Longevity Sciences, National Center for Geriatrics and Gerontology, Obu, Japan
[2]Department of Neurology, First Affiliated Hospital, China Medical University, Shenyang, P.R. China

Microglia are the main resident immunocompetent and phagocytic cells in the central nervous system (CNS). Activated microglia could play phagocytic roles as well as mediate inflammatory processes in the CNS. Involvement of activated microglia in the pathogenesis has been demonstrated in several neurological diseases including Alzheimer's disease (AD). Juzen-taiho-to (JTT), a traditional herbal medicine, has been reported to have effects on activating immune responses and phagocytosis. So far, little is known about the effects of this Kampo formulation JTT on microglia and in AD. In this report, we studied the effects of JTT on the activation and phagocytic functions of mouse microglia and bone marrow-derived macrophages (BMM). JTT could activate microglia, which was confirmed by the prominent morphological change and increased surface expression of an activation marker CD11b. In addition, JTT was revealed to induce microglial proliferation, and enhance microglial phagocytosis of, without eliciting an excessive production of nitric oxide. Furthermore, when mice were administrated with JTT in vivo, their BMM showed more effective phagocytosis of fibrillar $A\beta_{1\text{-}42}$. These findings implicate the therapeutic potential of JTT in AD and other neurological diseases accompanied by microglial activation. ——— Juzen-taiho-to (JTT); microglia/macrophages; Alzheimer's disease (AD); phagocytosis; amyloid.
Tohoku J. Exp. Med., 2008, **215** (1), 43-54.

Microglia are considered resident immune cells of myeloid origin, that take up residence in the central nervous system (CNS) during embryogenesis (Cuadros and Navascues 1998). They are regarded as CNS macrophages, and many studies gave evidence that immune reaction and inflammation related with microglia play essential roles in the pathological mechanism of some neurodegenerative diseases such as Alzheimer's disease (AD), multiple sclerosis, and so on (Rogers et al. 1988; Raine 1994). Activated microglia have been demonstrated to play the phagocytic role with extracellular β-amyloid deposits in AD (Kopec and Carroll 1998; Weldon et al. 1998). Therefore, microglia might be a therapeutic target for AD.

Juzen-taiho-to (Shi-Quan-Da-Bu-Tang in Chinese, JTT), a traditional herbal medicine, has traditionally been administered to patients with anemia, anorexia, or fatigue. From the pharmaco-

Received February 18, 2008; revision accepted for publication March 12, 2008.
Correspondence: Takeshi Tabira, National Institute for Longevity Sciences, National Center for Geriatrics and Gerontology, 36-3 Genko, Morioka, Obu 474-8511, Japan.
e-mail: tabira@nils.go.jp

logic view, JTT contains various immunomodulatory substances. For example, ginsenoside Rh1 has anti-allergic and anti-inflammatory activities (Park et al. 2004); glycyrrhizin extracted from Glycyrrhizae Radix and the extracts of Astragali Radix have anti-inflammatory activities (Shon and Nam 2003; Matsui et al. 2004); the extracts from Ginseng Radix, Cinnamomi Cortex, Glycyrrhizae Radix, Radix Paeoniae, and Astragali Radix have anti-oxidative activities (Dhuley 1999; Baltina 2003; Keum et al. 2003; Lee et al. 2003; Wang et al. 2003). Furthermore, recent studies demonstrated that ginsenosides Rg3 and Rh2 inhibited the production of nitric oxide (NO), iNOS and pro-inflammatory cytokines TNF-α, IL-1β in activated microglia (Bae et al. 2006). These results raised the possibility that the Kampo formulation JTT might have an immunomodulatory effect on microglia/macrophages, and might show its therapeutic potential in neurodegenerative diseases accompanied by microglial activation, such as AD.

In this study, we examined the effects of JTT on the activation and phagocytic functions of microglia and bone marrow-derived macrophages (BMM), as well as its effects on the production of NO in microglia.

Materials and Methods

Reagents

Synthetic human $A\beta_{1-42}$ peptide was purchased from Peptide Institute, Inc. (Osaka). Fibrillar $A\beta_{1-42}$ ($fA\beta_{42}$) was obtained by dissolving the synthetic human peptide firstly in DMSO and then in Dulbecco's PBS (250 μM) followed by incubating at 37°C for 7 days. Lipopolysaccharide (LPS) from Escherichia coli 055: B5 was purchased from Sigma-Aldrich (St. Louis, MO, USA). Fluorescein isothiocyanate (FITC)-conjugated rat anti-mouse CD11b monoclonal antibody was purchased from BD Biosciences Pharmingen (San Jose, CA, USA). Rabbit anti-Iba1 (ionized calcium binding adaptor molecule 1) polyclonal antibody was purchased from Wako Pure Chemicals Industries, Inc. (Osaka). Mouse anti-human $A\beta$ monoclonal antibody: 4G8 was purchased from Chemicon International, Inc. (Temecula, CA, USA). Rabbit anti-Lysosome-associated membrane protein (LAMP)-2 polyclonal antibody was purchased from Santa Cruz Biotechnology, Inc. (Santa Cruz, CA, USA). Recombinant mouse granulocyte macrophage-colony stimulating factor (GM-CSF) and recombinant mouse macrophage-colony stimulating factor (M-CSF) were from R & D Systems (Minneapolis, MN, USA).

Preparation of JTT

JTT, purchased from Tsumura and Co. (Tokyo), was composed of 10 medical plants (Table 1). JTT was prepared as follows. A mixture of Astragali Radix (3.0 g), Cinnamomi Cortex (3.0 g), Angelicae Radix (3.0 g), Paeoniae Radix (3.0 g), Cnidii Rhizoma (3.0 g), Rehmanniae Radix (3.0 g), Ginseng Radix (3.0 g), Atractylodis Lanceae Rhizoma (3.0 g), Poria (3.0 g), and Glycyrrhizae Radix (1.5 g) was added to 285 ml of water and extracted at 100°C for 1 hr. The extracted solution was filtered and spray-dried to obtain the dry extract powder (2.3 g).

Table 1. The ratio of crude drugs of Juzen-taiho-to (JTT)

Crude drugs	Ratio
Astragali Radix (*root of Astragalus membranaceus Bunge*)	3.0
Cinnamomi Cortex (*bark of Cinnamomum cassia Blume*)	3.0
Angelicae Radix (*root of Angelica acutiloba Kitagawa*)	3.0
Paeoniae Radix (*rhizome of Paeonia lactiflora Pallas*)	3.0
Cnidii Rhizoma (*rhizome of Cnidium officinale Makino*)	3.0
Rehmanniae Radix (*root of Rehmannia glutinosa Liboschitz var. purpurea Makino*)	3.0
Ginseng Radix (*root of Panax ginseng C.A. Meyer*)	3.0
Atractylodis Lanceae Rhizoma (*rhizome of Atractylodes lancea De Candolle*)	3.0
Poria (*scletrotium of Poria cocos Wolf*)	3.0
Glycyrrhizae Radix (*root of Glycyrrhiza uralensis Fischier*)	1.5

Preparation of the JTT mixture culture medium

JTT extract powder was dissolved in Dulbecco's Modified Eagle's Medium (DMEM, Sigma) by stirring at room temperature for 1 hr at a concentration of 2 mg/ml. After dissolved, it was sonicated for 30 min (Branson Sonifier 250, Danbury, CT, USA), and centrifuged at 3,000 rpm for 10 min (J6-HC Centrifuge, Beckman Coulter, Fullerton, CA, USA) to remove the insoluble materials. The supernatant was then filtered with a disposable syringe filter with a 0.22 μm PVDF membrane (Millipore, Cork, Ireland). This solution was then added with 10% fetal bovine serum (FBS, ICN Biomedicals, Aurora, OH, USA), 0.2% glucose and 5 μg/ml bovine insulin to prepare the JTT mixture culture medium.

Preparation and culture of primary microglia and Ra2 cell lines

Mouse primary microglia were isolated from primary mixed glial cell cultures obtained from newborn C57BL/6 mice by the "shaking off" method as described previously (Suzumura et al. 1987). In brief, after the meninges were carefully removed under microscope, the brains were dissociated by passing it through a 258-μm-pore nylon mesh. The cell suspension was washed twice with Hank's balanced salt solution, triturated and placed in 75-cm^2 culture flasks at a density equivalent of two brains per flask in 10 ml DMEM supplemented with 10% FBS, 0.2% glucose and 5 μg/ml bovine insulin. On the 14th day, the mixed glial cell cultures were put into Bio Shaker (TAITEC, BR-43FM, Koshigaya), and were shaken at 37°C, 150 rpm for 3 hrs. The medium was collected, centrifuged, and the harvested cells were incubated at 37°C, 5% CO_2 for 30 min. The attached cells were harvested by cell scraper. The morphological change was observed under an Olympus IX70 microscope (Olympus, Tokyo) and recorded with a Nikon digital camera DXM1200F (Nikon, Tokyo). The purity of cultured microglia was 97-100% as determined by indirect immunofluorescence staining with antibody to Iba1.

The microglial cell line Ra2 cells established from neonatal C57BL/6J (H-2^b) mice using a non-enzymatic and non-virus-transformed procedure (Sawada et al. 1998) were kindly provided by Dr. Sawada (Department of Brain Function, Research Institute of Environmental Medicine, Nagoya University, Nagoya). Ra2 cells proliferated in the same culture medium as primary microglia supplemented with 1 ng/ml GM-CSF. Before experiment, the Ra2 cells were cultured without GM-CSF for 16 hrs.

Preparation and culture of bone marrow-derived macrophages (BMM)

12-week-old female C57BL/6 wild type mice were used in this experiment. This experiment was performed under the guidelines for Animal Experiments of National Center for Geriatrics and Gerontology and approval of the institute's ethical committee for animal experiment. 8 mice were randomly divided into two groups. One group (experimental group, n = 4) was given drinking water containing 100 mg/ml of JTT. The dose was determined according to our previous study (Hara et al. unpublished). The drinking water was prepared by the similar protocol with the preparation of JTT mixture culture medium mentioned above. Since 20% of JTT was removed by the procedure of sedimentation during the preparation and each animal consumed 3 ml of the drinking water per day, the average consumption of JTT was estimated as 250 mg/day/caput. If animals spill over about 20% of drinking water, this is about 100 times higher than the dosage for human use. The other group (control group, n = 4) was given plain drinking water. After 21 days, isolation of BMM was performed by a modified method published by Takahashi and collaborators (Takahashi et al. 2007). In detail, the mice were sacrificed by decapitation and bone marrow cells were freshly flushed from the medullary cavities of the femurs and tibias with a 25 ga needle, and then filtered through a 40 μm nylon mesh. Removal of erythrocytes was performed by lysis with hypotonic solution, followed by washing twice with Dulbecco's PBS containing 2% FBS. The cells were then resuspended in DMEM containing 10% FBS and 10 ng/ml M-CSF in 75-cm^2 culture flasks. After 24 hrs, non-adherent cells were collected and re-seeded in fresh 75-cm^2 culture flasks. Medium was changed every three days, and BMM were collected for fAβ_{42}-phagocytosis assay after 12 - 13 days. The purity of BMM was more than 95% as determined by indirect immunofluorescence staining with antibody to Iba1.

Cell proliferation (WST-1) assay

Primary microglia at a density of 2 × 10^4 cells/well were plated onto a 96-well microtiter plate. Different concentrations of JTT (10, 50, 100, 200, 400 and 600 μg/ml) or LPS (0.1 μg/ml) as positive control were added to the culture medium for 48 hrs. Cell proliferation assay was determined by the PreMix WST-1 cell proliferation assay system (TaKaRa, Tokyo). This assay bases on the cleavage of tetrazolium salts which were added into the medium. These teterazolium salts are cleaved to forma-

zan dye by succinate-tetrazolium reductase, which exists in the mitochondrial respiratory chain and is active only in viable cells. At the end of the experiments, 10 μl/well PreMix WST-1 reagent was added followed by incubating at 37°C, 5% CO_2 for 4 hrs. The absorbance at the wavelength of 450 nm was measured by a microplate reader (model 550, Bio-Rad Laboratories, Hercules, CA, USA).

Flow cytometric assay

Ra2 cells were treated with different concentrations of JTT (200 and 400 μg/ml) or LPS (0.1 μg/ml) for 48 hrs. The cells were detached and single cell suspensions were made in fluorescence activated cell sorting (FACS) buffer consisting of Dulbecco's PBS containing 4% FBS and 0.1% sodium azide. The cells were then incubated with FITC-conjugated rat anti-mouse CD11b monoclonal antibody for cell surface staining at 4°C for 30 min. After washed twice with FACS buffer to remove the antibody completely, the samples were examined by FACSCalibur flow cytometer (BD, Franklin Lakes, NJ, USA) and analyzed using the Cellquest^{TM} software (BD immunocytometry system, CA, USA).

Immunofluorescence staining for fAβ_{42}-phagocytosis assay

Both primary microglia in vitro pre-treated with different concentrations of JTT (100, 200, 400 or 600 μg/ml) for 24 hrs or pre-treated with 200 μg/ml JTT for different time periods (12, 24 or 48 hrs) and BMM from two groups which were in vivo pre-administrated with or without 100 mg/ml JTT were used for fAβ_{42}-phagocytosis assay. At the end of each treatment, the culture medium was changed and fAβ_{42} was added to a final concentration of 1 μM, followed by incubation for further 3 hrs. After fixation with 4% paraformaldehyde at 4°C for 15 min, the cells were blocked and permeabilized with PBS containing 5% normal donkey serum, 0.5% bovine serum albumin and 0.2% Triton X-100 at room temperature for 1 h. Microglia or BMM were then stained with anti-Iba1 antibody (1 : 250) or anti-LAMP-2 antibody (1:250), and fAβ_{42} was stained with 4G8 antibody (1:500) at 4°C overnight. After 3-time washes with PBS, specific binding was detected using secondary antibodies: Alexa 488-conjugated donkey anti-rabbit IgG and Alexa 594-conjugated donkey anti-mouse IgG (Molecular Probes, Eugene, OR, USA). After washing, the fluorescence was observed by an Olympus IX70 microscope equipped with appropriate filters. The fAβ_{42}-phagocytosed microglia in each group were counted in at least three randomly chosen areas containing more than 200 Iba1 or LAMP-2 positive cells under fluorescence microscope as the total cell numbers. When stained with anti-Iba1 antibody, the numbers of microglia containing engulfed fAβ_{42} were determined by counting cells with Alexa 594 internalization around nuclei other than on the cell surface. When stained with anti-LAMP-2 antibody, the numbers of microglia containing engulfed fAβ_{42} were determined by counting cells with the colocalization of Alexa 488 and Alexa 594 fluorescence. The percentages of fAβ_{42}-phagocytosed microglia pre-treated with different concentrations of JTT were shown as means and standard deviation (S.D.) from three independent experiments with Iba1 and 4G8 staining and one experiment with LAMP-2 and 4G8 staining. While the percentages of fAβ_{42}-phagocytosed microglia pre-treated with 200 μg/ml JTT for different time periods were shown as means and SD from three independent experiments with Iba1 and 4G8 staining. The percentages of fAβ_{42}-phagocytosed BMM were analyzed similarly from four mice per group with Iba1 and 4G8 staining.

Nitric oxide (NO) quantification

The Griess reaction is extensively used as an indicator of NO production by cultured cells. Primary microglia were plated on 48-well culture plates at 1×10^5 cells/well, and treated with or without 200 μg/ml JTT for 24 hrs. Afterwards, the culture medium was changed with or without 10 μM fAβ_{42} for another 24 hrs incubation. The media collected were centrifuged and the cell-free supernatants were then quantitatively determined for total NO production using a total NO assay kit (Endogen, Pierce Biotechnology, Rockford, IL, USA). The assay was carried out according to the manufacturer's protocol.

Statistical analyses

All results were expressed as means ± S.D. The statistical significance of differences was determined by two-tailed Student's *t*-test or analysis of variance (ANOVA) followed by the post-hoc multiple comparison.

RESULTS

Effects of JTT on the morphological change of microglial activation

The effect of JTT on microglial activation was first revealed by observing prominent morphological changes of primary microglia treated with JTT under the phase contrast microscope. It

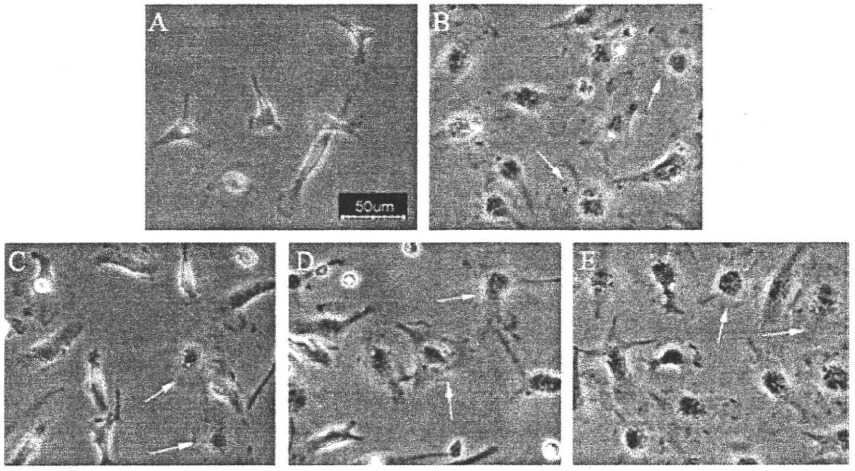

Fig. 1. JTT changed the morphological appearance of primary microglia. Primary microglia were cultured for 24 hrs in (A) unstimulated condition, (B) LPS (0.1 μg/ml), (C) JTT (100 μg/ml), (D) JTT (200 μg/ml), and (E) JTT (400 μg/ml) and observed under the phase contrast microscope. The arrows show some of the activated microglia with amoeboid morphology. Scale bar, 50 μm.

is well known that resting microglia adopt a characteristic highly ramified and elongated morphological appearance with small cell bodies, while activated microglia undergo dramatic morphological changes showing amoeboid morphology with large cell bodies and short processes (Kreutzberg 1996). When we treated primary microglia with different concentrations of JTT or LPS for 24 hrs, we observed that they showed obvious activated morphological appearance, particularly in 200 and 400 μg/ml JTT-treated groups (Fig. 1).

Effect of JTT on microglial proliferation and viability

To investigate the possible role of JTT in the proliferation and activation of microglia, next we examined whether JTT could sustain the cell proliferation of primary microglia by the WST-1 assay. As expected, JTT increased microglial proliferation and viability in a slightly dose-dependent fashion. Compared with LPS, JTT showed similar or more promoting effects on microglial proliferation and viability (Fig. 2). From this result and the above morphological change result, we chose the concentrations of 200 and 400 μg/ml for some of the following experiments.

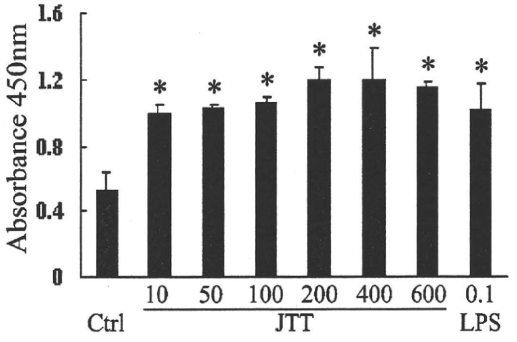

Fig. 2. JTT induced cell proliferation of primary microglia by the WST-1 cell proliferation assay. Primary microglia were seeded at a density of 2×10^4 cells/well in a 96-well microtiter plate as described in the Materials and Methods. After treatment with different concentrations of JTT as well as LPS as a positive control for 48 hrs, the cultures were added with the WST-1 reagent followed by 4 hrs incubation, and then the absorbance at 450 nm was measured. Mean ± S.D. values from a single experiment were obtained in triplicate. Similar results were obtained in two separate experiments. $*p < 0.01$ vs control group (unstimulated condition) analyzed by Dunnett's test in ANOVA.

Effect of JTT on the surface expression of CD11b

The flow cytometric assay was used to check the expression of surface marker CD11b on microglial cell line Ra2, which indicates the activation of microglia. Ra2 cells have been confirmed to have similar properties to primary microglia, and have been generally used as the substitutes of primary microglia in experimental research (Ito et al. 2005, 2006; Laquintana et al. 2007; Roepstorff et al. 2007). Ra2 cells were used in the flow cytometric assay because they showed easily-detached property after treatment than primary microglia. So Ra2 cells were more suitable for this assay in order to obtain more creditable results. Two peaks were obtained apparently in every treated group but not in an unstimulated condition after either 24 or 48 hrs treatment, indicating that the latter peak should be formed by activated cells (M1). After 24 hrs treatment with JTT or LPS, the percentage of activated cell number and their mean fluorescence intensity (mFI) were both increased compared to the negative control group, but there was no significant difference (data not shown). However, after 48 hrs treatment, there was significant difference when the above two indexes were analyzed, while there was no difference between the 200 and 400 μg/ml JTT treatment groups (Fig. 3). JTT increased the cell number percentage and mFI of M1 by about 50% and 170%, respectively, relative to the negative control. These results

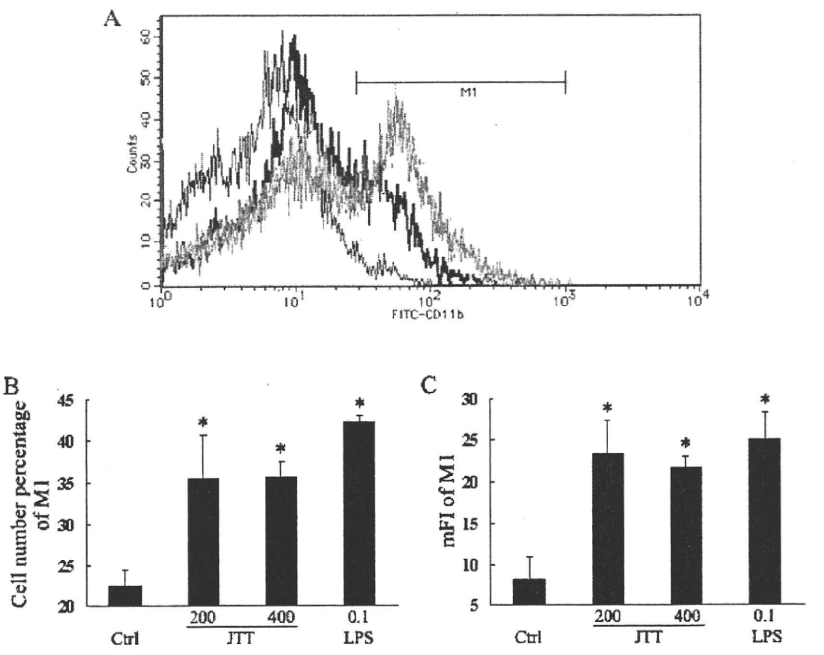

Fig. 3. JTT increased the surface expression of CD11b. Ra2 microglial cells were treated with 200, 400 μg/ml JTT or 0.1 μg/ml LPS for 48 hrs as described in the Materials and Methods. After gently detached, Ra2 cells were stained with FITC-conjugated anti-CD11b antibody for the FACS analysis. (A) Overlay of flow cytometry histograms of untreated cells without staining (gray line), untreated cells as control (black line), 200 μg/ml JTT-treated cells (red line), 400 μg/ml JTT-treated cells (yellow line) and LPS-treated cells (green line). M1, which referred to the second peak, represents the activated cells whose CD11b expression was increased. (B) The cell number percentage of M1 in each group. (C) Mean fluorescence intensity of M1 in each group. Mean ± S.D. values from a single experiment were performed in triplicate. Similar results were obtained in two independent experiments. $^*p < 0.01$ vs control group analyzed by Dunnett's test in ANOVA.

confirmed that JTT could induce the surface expression of an activation marker CD11b on microglia, but it might take at least 48 hrs to show this effect.

Effect of JTT on Microglial Phagocytosis of fAβ_{42}

Since the above findings confirmed that JTT could induce the proliferation and activation of microglia, we next examined whether JTT could enhance microglial phagocytosis of fAβ_{42}. We could see that JTT did enhance the microglial phagocytosis of fAβ_{42} obviously after 24 hrs treatment when the concentration of JTT was higher than 200 μg/ml, but did not show a concentration-dependent fashion (Fig. 4E). The 200 μg/ml JTT-treated group got the highest percentage of phagocytosed cells of 60.5 ± 5.4%, which is higher than the negative control (33.7 ± 4.4%) and the LPS positive control (46.9 ± 2.3%) by 26.8 ± 1.3% and 13.6 ± 6.2%, respectively. To examine whether the effect of JTT showed time-dependent fashion, 200 μg/ml JTT was used to treat primary microglia for different time periods. The 24 hrs treatment group showed the highest percentage of phagocytosed cells of 60.4 ± 4.4%. No evident time-dependent fashion was seen as shown in Fig. 4F.

Effect of JTT on BMM phagocytosis of fAβ_{42}

The fAβ_{42} phagocytosis was also investigated in BMM in this study. The BMM from the two groups (four mice each) which had been pre-administrated with or without JTT were cultured for 12 - 13 days as described above, and then their ability of fAβ_{42} phagocytosis was examined using

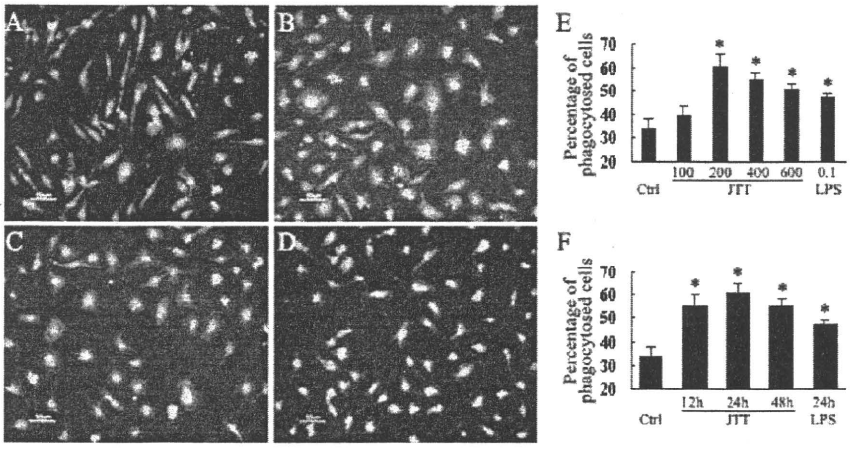

Fig. 4. JTT enhanced the phagocytosis of fAβ_{42} in primary microglia. Primary microglia were treated with JTT or LPS. Then the culture medium was changed and 1 μM fAβ_{42} was added for further 3 hrs incubation followed by immunofluorescence double staining as described in the Materials and Methods. (A-D) The cells were stained with antibodies directed against Iba1 and 4G8, and then with Alexa 488 (green) and Alexa 594 (red)-conjugated secondary antibodies, respectively. Under fluorescence microscope, colocalization of microglia and fAβ_{42} was shown by yellow color as a result of superimposing fluorescence images of microglia (green) and fAβ_{42} (red). (A) Control (unstimulated condition, 24 hrs). (B) JTT (200 μg/ml, 24 hrs). (C) JTT (400 μg/ml, 24 hrs). (D) LPS (0.1 μg/ml, 24 hrs). (E) Microglia were treated with different concentrations of JTT or LPS for 24 hrs. Percentages of phagocytosed cells were counted. Mean ± S.D. values were obtained from three separate experiments with Iba1 and 4G8 staining and one experiment with LAMP-2 and 4G8 staining (figure not shown). (F) Microglia were treated with 200 μg/ml JTT for distinct time periods (12, 24, 48 hrs) or 0.1 μg/ml LPS for 24 hrs. Percentages of phagocytosed cells were counted (figure not shown). Mean ± S.D. values were obtained from three separate experiments with Iba1 and 4G8 staining. Scale bars represent 50 μm. *$p < 0.01$ vs control group analyzed by Dunnett's test in ANOVA.

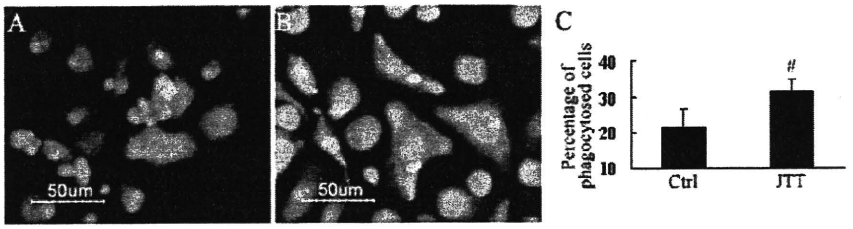

Fig. 5. JTT enhanced the phagocytosis of fAβ_{42} in BMM. BMM were obtained from mice with or without JTT administration and cultured for about 2 weeks. Then the culture medium was changed and 1 μM fAβ_{42} was added for further 3 hrs incubation followed by immunofluorescence double staining as described in the Materials and Methods. (A-B) The cells were stained with antibodies directed against Iba1 and 4G8, and then with Alexa 488 (green) and Alexa 594 (red)-conjugated secondary antibodies, respectively. Under fluorescence microscope, colocalization of BMM and fAβ_{42} was shown by yellow color as a result of superimposing fluorescence images of BMM (green) and fAβ_{42} (red). (A) Control group (without JTT administration), (B) JTT administration group, (C) Percentages of phagocytosed cells. Mean ± S.D. values were obtained from four mice. Scale bars represent 50 μm. #$p < 0.05$ vs control group analyzed by two-tailed Student's t test.

immunofluorescence double staining according to the same protocol mentioned above. As shown in Fig. 5, some BMM from JTT-administrated mice showed larger cell bodies and stronger signal of Iba1 staining (Fig. 5B) compared to the control group (Fig. 5A), as well as the higher percentage of fAβ_{42}-phagocytosed cells (31.6 ± 3.3% vs 21.6 ± 5.2%, respectively, $p < 0.05$) (Fig. 5C).

Effect of JTT on NO production in primary microglia

The effect of JTT treatment on NO production in primary microglia was investigated by the Griess reaction. The ratio of NO production to the control group was shown in Fig. 6. Twenty hundred μg/ml JTT was used to treat primary microglia. It slightly increased NO production but no statistical difference compared to the control group ($p = 0.396$), but LPS or 10 μM fAβ_{42} did increase ($p = 0.000$ and 0.008, respectively). And between the JTT and LPS groups, there was also significant difference ($p = 0.002$). In the presence of 10 μM fAβ_{42}, although JTT treatment did not reduce the NO production, at least it did not increase the NO production ($p = 0.396$).

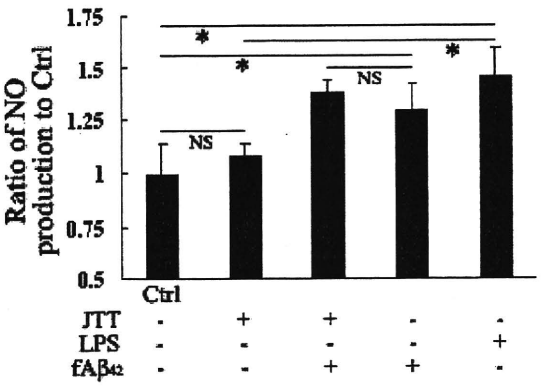

Fig. 6. JTT did not increase the production of NO in primary microglia. Primary microglia were treated with 200 μg/ml JTT or 0.1 μg/ml LPS for the first 24 hrs, then the culture was continued with or without 10 μM fAβ_{42} for another 24 hrs. The supernatants were obtained and their contents of NO were measured by the Griess reaction as described in the Materials and Methods. The ratios of NO production of each group to the control group (untreated condition) were shown. Mean ± S.D. values were obtained from a single experiment in triplicate. Similar results were obtained in two separate experiments. *$p < 0.01$ analyzed by least significant difference test in ANOVA. NS, not significant.

Discussion

Microglia represent the brain innate immune system and hence the first line of defense against

invading pathogens and serve as specialized sensors for brain tissue injury (Streit et al. 2005; Conde and Streit 2006). Under pathological situations, such as neurodegenerative disease, microglia become activated, migrate to and surround damaged or dead cells, and subsequently clear cellular debris from the area, similar to the phagocytic active macrophages of the peripheral immune system (Fetler and Amigorena 2005). At the same time, activated microglia are also revealed to produce NO and some kinds of pro-inflammatory cytokines, which are considered to enhance the inflammation and exacerbate the diseases. There is considerable debate as to whether activated microglia are beneficial or harmful in AD. This may, however depend on the degree of activation. Nowadays, many researchers focused on how to inhibit microglial activation to restrain the inflammation. But it should also be noted that activated microglia are able to reduce Aβ accumulation by increasing its phagocytosis, clearance and degradation (Frautschy et al. 1998; Qiu et al. 1998; Yan et al. 2003). While an exaggerated immune response can certainly be detrimental to the CNS, increasing evidence demonstrates that a controlled inflammatory reaction in the brain can be greatly beneficial to the health and proper function of the CNS. So in the present study, we attempted to search a way through which we can make a controlled activation of microglia.

Among more than one hundred kinds of herbal medicines, JTT is well known to enhance the immunological functions (Matsumoto et al. 2000). Nowadays, since its anti-cancer effects (Dai et al. 2001; Tagami et al. 2004) and suppressive effects on toxicity of anti-cancer drugs (Sugiyama et al. 1995a, b) were confirmed, JTT is often clinically used for the treatment of cancer patients. And JTT has also been demonstrated to have influence not only on the acquired immune system but also the innate immune response related with macrophages (Chino et al. 2005). In the neurological diseases, AD has been demonstrated to be highly related with immune response and inflammation. Preliminary results from in vivo experiment in our laboratory supported that JTT administration diminished the senile plaques in AD transgenic mouse (Hara et al. unpublished observation). These findings prompted us to clarify the possible mechanism of the diminishing of senile plaques in order to search a new possible therapeutic way for AD.

First, we treated naive primary microglia with different concentrations of JTT, a dramatic morphological change from resting ramified cells to amoeboid microglia was observed, as well as decreased refraction and better adherent property, obviously in 200 and 400 μg/ml groups. This finding encouraged us to detect whether JTT activated microglia definitely.

Then the fact that JTT did activate microglia was demonstrated by the WST-1 cell proliferation assay and flow cytometric assay to check the surface expression of an activation marker CD11b. From the cell proliferation assay, JTT increased microglial proliferation and viability even though at a low concentration (10 μg/ml) with a slight concentration-dependent fashion. In the flow cytometric analysis, CD11b, a well-known activation marker of microglia/macrophages, was used. As expected, two peaks appeared obviously, similar with the LPS-treated group, indicating that the second peak represented the activated cells. These findings revealed that the Kampo formulation JTT could induce microglial proliferation and activation.

Then, important in our experiment was the phagocytosis-enhancing effect of JTT. There are very limited reports about phagocytosis-enhancing effects using crude extracts or oral administration of herbal medicine. According to the previous report (Liu et al. 2005), phagocytosis might be dissociated from inflammatory microglial activation in relation to the AD stage. So in the fAβ_{42}-phagocytosis assay, we chose a low (1 μM) fAβ_{42} concentration. Although 100 μg/ml JTT induced microglial proliferation, it showed no significant effect on fAβ_{42}-phagocytosis (p = 0.171); while 200 μg/ml JTT treatment increased the percentage of phagocytosed cells by about 80% compared to the unstimulated group, indicating that to show phagocytosis-enhancing effect, a relatively higher concentration was needed than to induce microglial proliferation. This concen-

tration of 200 μg/ml in in vitro experiments was consistent with the dosage for human use and the previous reports about the in vitro studies of JTT (Hisha et al. 1997; Kamiyama et al. 2005). Although 12 hrs treatment was enough to enhance the phagocytosis, no time-dependent fashion was detected. In recent studies, more attention was paid on the effect of bone marrow-derived microglia on restricting senile plaque formation (Malm et al. 2005; Simard et al. 2006). In this study, using M-CSF, we induced the bone marrow stem cells or myeloid progenitor cells to differentiate to macrophages, and we found that orally administrated JTT could also enhance the phagocytosis of f$A\beta_{42}$ in BMM. However, we used a dose of 100 mg/ml according to our previous protocol. As mentioned above, this is much higher than the dosage for human use. Although animals were tolerated well with the dose, we need to repeat the experiment with lower doses.

Activated microglia can produce NO and other pro-inflammatory cytokines, most of which are considered to be detrimental to neurons, and play an important role in the pathogenesis of AD. Excessive production of NO can mediate oxidative stress as well as amplify inflammation cascade reactions. Here we examined the NO production as a representative index. In this assay, a relatively higher (10 μM) f$A\beta_{42}$ concentration was used. First, JTT treatment did not increase the NO production, but LPS and f$A\beta_{42}$ did. Second, in the presence of f$A\beta_{42}$, although JTT pre-treatment did not reduce the NO production, at least it did not increase NO. This finding and the above results indicated that with proper concentrations and time periods of treatment, JTT might induce activation and mediate phagocytosis without eliciting excessive production of neurotoxic NO in microglia/macrophages.

In summary, the results of this study demonstrated that Kampo formulation JTT could induce microglial proliferation and activation, and also enhance f$A\beta_{42}$-phagocytosis in microglia and BMM without excessive NO production. To our knowledge, this is the first report indicating that JTT has enhancing effect of f$A\beta_{42}$-phagocytosis on microglia/macrophages. These findings support our previous finding that JTT administration diminished the senile plaque in AD transgenic mouse, which might be due to the enhanced phagocytosis of Aβ by microglia, and the phagocytosis-enhancing effect of JTT might not be accompanied by excessive inflammatoty mediators' production. This is also consistent with the previous reports showing the anti-inflammatory and anti-oxidative activities of the components of JTT (Lee et al. 2003; Matsui et al. 2004). These findings suggest that JTT administration would be a potential therapeutic or preventive approach for AD. Further intensive study should be performed in order to evaluate its therapeutic effect by in vivo study and to elucidate the underline mechanism in detail.

Acknowledgments

This study was partially supported by Grant-in-Aid for Scientific Research on Priority Areas (17025056) from the Ministry of Education, Culture, Sports, Science and Technology. Huayan Liu is a fellow supported by Sasakawa Foundation. We thank Sasakawa Memorial Health Foundation and Japan China Medical Association for their kind support. We also thank Dr. A. Suzumura, M. Sawada, K. Takahashi, H. Wakita, A. Watanabe, S. Kataoka, K. Adachi, K. Yoshizaki, and K. Takeda for their kind help and discussion in this work.

References

Bae, E.A., Kim, E.J., Park, J.S., Kim, H.S., Ryu, J.H. & Kim, D.H. (2006) Ginsenosides Rg3 and Rh2 inhibit the activation of AP-1 and protein kinase A pathway in lipopolysaccharide/ interferon-γ-stimulated BV-2 microglial cells. *Planta. Med.*, **72**, 627-633.

Baltina, L.A. (2003) Chemical modification of glycyrrhizic acid as a route to new bioactive compounds for medicine. *Curr. Med. Chem.*, **10**, 155-171.

Chino, A., Sakurai, H., Choo, M.K., Koizumi, K., Shimada, Y., Terasawa, K. & Saiki, I. (2005) Juzentaihoto, a Kampo medicine, enhances IL-12 production by modulating Toll-like receptor 4 signaling pathways in murine peritoneal exudate macrophages. *Int. Immunopharmacol.*, **5**, 871-882.

Conde, J.R. & Streit, W.J. (2006) Microglia in the aging brain. *J. Neuropathol. Exp. Neurol.*, **65**, 199-203.

Cuadros, M.A. & Navascues, J. (1998) The origin and differentiation of microglial cells during development. *Prog. Neurobiol.*, **56**, 173-189.

Dai, Y., Kato, M., Takeda, K., Kawamoto, Y., Akhand, A.A., Hossain, K., Suzuki, H. & Nakashima, I. (2001) T-cell-immunity-based inhibitory effects of orally administered herbal medicine juzen-taiho-to on the growth of primarily developed melanocytic tumors in RET-transgenic mice. *J. Invest. Dermatol.*, **117**, 694-701.

Dhuley, J.N. (1999) Anti-oxidant effects of cinnamon (Cinnamomum verum) bark and greater cardamom (Amomum subulatum) seeds in rats fed high fat diet. *Indian. J. Exp. Biol.*, **37**, 238-242.

Fetler, L. & Amigorena, S. (2005) Neuroscience. Brain under surveillance: the microglia patrol. *Science*, **309**, 392-393.

Frautschy, S.A., Yang, F., Irrizarry, M., Hyman, B., Saido, T.C., Hsiao, K. & Cole, G.M. (1998) Microglial response to amyloid plaques in APPsw transgenic mice. *Am. J. Pathol.*, **152**, 307-317.

Hisha, H., Yamada, H., Sakurai, M.H., Kiyohara, H., Li, Y., Yu, C., Takemoto, N., Kawamura, H., Yamaura, K., Shinohara, S., Komatsu, Y., Aburada, M. & Ikehara, S. (1997) Isolation and identification of hematopoietic stem cell-stimulating substances from Kampo (Japanese herbal) medicine, Juzen-taiho-to. *Blood*, **90**, 1022-1030.

Ito, S., Sawada, M., Haneda, M., Fujii, S., Oh-Hashi, K., Kiuchi, K., Takahashi, M. & Isobe, K. (2005) Amyloid-β peptides induce cell proliferation and macrophage colony-stimulating factor expression via the PI3-kinase/Akt pathway in cultured Ra2 microglial cells. *FEBS. Lett.*, **579**, 1995-2000.

Ito, S., Sawada, M., Haneda, M., Ishida, Y. & Isobe, K. (2006) Amyloid-beta peptides induce several chemokine mRNA expressions in the primary microglia and Ra2 cell line via the PI3K/Akt and/or ERK pathway. *Neurosci. Res.*, **56**, 294-299.

Kamiyama, H., Takano, S., Ishikawa, E., Tsuboi, K. & Matsumura, A. (2005) Anti-angiogenic and immunomodulatory effect of the herbal medicine "Juzen-taiho-to" on malignant glioma. *Biol. Pharm. Bull.*, **28**, 2111-2116.

Keum, Y.S., Han, S.S., Chun, K.S., Park, K.K., Park, J.H., Lee, S.K. & Surh, Y.J. (2003) Inhibitory effects of the ginsenoside Rg3 on phorbol ester-induced cyclooxygenase-2 expression, NF-κB activation and tumor promotion. *Mutat. Res.*, **523-524**, 75-85.

Kopec, K.K. & Carroll, R.T. (1998) Alzheimer's β-amyloid peptide 1-42 induces a phagocytic response in murine microglia. *J. Neurochem.*, **71**, 2123-2131.

Kreutzberg, G.W. (1996) Microglia: a sensor for pathological events in the CNS. *Trends. Neurosci.*, **19**, 312-318.

Laquintana, V., Denora, N., Lopedota, A., Suzuki, H., Sawada, M., Serra, M., Biggio, G., Latrofa, A., Trapani, G. & Liso, G. (2007) *N*-Benzyl-2-(6,8-dichloro-2-(4-chlorophenyl) imidazo [1,2-*a*] pyridin-3-yl)-*N*-(6-(7-nitrobenzo [*c*] [1,2,5] oxadiazol-4-ylamino) hexyl) acetamide as a new fluorescent probe for peripheral benzodiazepine receptor and microglial cell visualization. *Bioconjug. Chem.*, **18**, 1397-1407.

Lee, S.J., Lee, I.S. & Mar, W. (2003) Inhibition of inducible nitric oxide synthase and cyclooxygenase-2 activity by 1,2,3,4,6-penta-O-galloyl-beta-D-glucose in murine macrophage cells. *Arch. Pharm. Res.*, **26**, 832-839.

Liu, Y., Walter, S., Stagi, M., Cherny, D., Letiembre, M., Schulz-Schaeffer, W., Heine, H., Penke, B., Neumann, H. & Fassbender, K. (2005) LPS receptor (CD14): a receptor for phagocytosis of Alzheimer's amyloid peptide. *Brain*, **128**, 1778-1789.

Malm, T.M., Koistinaho, M., Parepalo, M., Vatanen, T., Ooka, A., Karlsson, S. & Koistinaho, J. (2005) Bone-marrow-derived cells contribute to the recruitment of microglial cells in response to β-amyloid deposition in APP/PS1 double transgenic Alzheimer mice. *Neurobiol. Dis.*, **18**, 134-142.

Matsui, S., Matsumoto, H., Sonoda, Y., Ando, K., Aizu-Yokota, E., Sato, T. & Kasahara, T. (2004) Glycyrrhizin and related compounds down-regulate production of inflammatory chemokines IL-8 and eotaxin 1 in a human lung fibroblast cell line. *Int. Immunopharmacol.*, **4**, 1633-1644.

Matsumoto, T., Sakurai, M.H., Kiyohara, H. & Yamada, H. (2000) Orally administered decoction of Kampo (Japanese herbal) medicine, "Juzen-Taiho-To" modulates cytokine secretion and induces NKT cells in mouse liver. *Immunopharmacology*, **46**, 149-161.

Park, E.K., Choo, M.K., Han, M.J. & Kim, D.H. (2004) Ginsenoside Rh1 possesses antiallergic and anti-inflammatory activities. *Int. Arch. Allergy. Immunol.*, **133**, 113-120.

Qiu, W.Q., Walsh, D.M., Ye, Z., Vekrellis, K., Zhang, J., Podlisny, M.B., Rosner, M.R., Safavi, A., Hersh, L.B. & Selkoe, D.J. (1998) Insulin-degrading enzyme regulates extracellular levels of amyloid beta-protein by degradation. *J. Biol. Chem.*, **273**, 32730-32738.

Raine, C.S. (1994) Multiple sclerosis: immune system molecule expression in the central nervous system. *J. Neuropathol. Exp. Neurol.*, **53**, 328-337.

Roepstorff, K., Rasmussen, I., Sawada, M., Cudre-Maroux, C., Salmon, P., Bokoch, G., van Deurs, B. & Vilhardt, F. (2007) Stimulus dependent regulation of the phagocyte NADPH oxidase by a VAV1, rac1, and PAK1 signaling axis. *J. Biol. Chem.*, Epub ahead of print.

Rogers, J., Luber-Narod, J., Styren, S.D. & Civin, W.H. (1988) Expression of immune system-associated antigens by cells of the human central nervous system: relationship to the pathology of Alzheimer's disease. *Neurobiol. Aging*, **9**, 339-349.

Sawada, M., Imai, F., Suzuki, H., Hayakawa, M., Kanno, T. & Nagatsu, T. (1998) Brain-specific gene expression by immortalized microglial cell-mediated gene transfer in the mammalian brain. *FEBS. Lett.*, **433**, 37-40.

Shon, Y.H. & Nam, K.S. (2003) Protective effect of Astragali radix extract on interleukin 1β-induced inflammation in human amnion. *Phytother. Res.*, **17**, 1016-1020.

Simard, A.R., Soulet, D., Gowing, G., Julien, J.P. & Rivest, S. (2006) Bone marrow-derived microglia play a critical role in restricting senile plaque formation in Alzheimer's disease. *Neuron.*, **49**, 489-502.

Streit, W.J., Conde, J.R., Fendrick, S.E., Flanary, B.E. & Mariani, C.L. (2005) Role of microglia in the central nervous system's immune response. *Neurol. Res.*, **27**, 685-691.

Sugiyama, K., Ueda, H. & Ichio, Y. (1995a) Protective effect of juzen-taiho-to against carboplatin-induced toxic side effects in mice. *Biol. Pharm. Bull.*, **18**, 544-548.

Sugiyama, K., Ueda, H., Ichio, Y. & Yokota, M. (1995b) Improvement of cisplatin toxicity and lethality by juzen-taiho-to in mice. *Biol. Pharm. Bull.*, **18**, 53-58.

Suzumura, A., Mezitis, S.G., Gonatas, N.K. & Silberberg, D.H. (1987) MHC antigen expression on bulk isolated macrophage-microglia from newborn mouse brain: induction of Ia antigen expression by gamma-interferon. *J. Neuroimmunol.*, **15**, 263-278.

Tagami, K., Niwa, K., Lian, Z., Gao, J., Mori, H. & Tamaya, T. (2004) Preventive effect of Juzen-taiho-to on endometrial carcinogenesis in mice is based on Shimotsu-to constituent. *Biol. Pharm. Bull.*, **27**, 156-161.

Takahashi, K., Prinz, M., Stagi, M., Chechneva, Olga. & Neumann, H. (2007) TREM2- transduced myeloid precursors mediate nervous tissue debris clearance and facilitate recovery in an animal model of multiple sclerosis. *PLoS. Med.*, **4**, e124.

Wang, P., Zhang, Z., Ma, X., Huang, Y., Liu, X., Tu, P. & Tong, T. (2003) HDTIC-1 and HDTIC-2, two compounds extracted from Astragali Radix, delay replicative senescence of human diploid fibroblasts. *Mech. Ageing Dev.*, **124**, 1025-1034.

Weldon, D.T., Rogers, S.D., Ghilardi, J.R., Finke, M.P., Cleary, J.P., O'Hare, E., Esler, W.P., Maggio, J.E. & Mantyh, P.W. (1998) Fibrillar β-amyloid induces microglial phagocytosis, expression of inducible nitric oxide synthase, and loss of a select population of neurons in the rat CNS in vivo. *J. Neurosci.*, **18**, 2161-2173.

Yan, Q., Zhang, J., Liu, H., Babu-Khan, S., Vassar, R., Biere, A.L., Citron, M. & Landreth, G. (2003) Anti-inflammatory drug therapy alters beta-amyloid processing and deposition in an animal model of Alzheimer's disease. *J. Neurosci.*, **23**, 7504-7509.